AD NUMBER

AD235384

LIMITATION CHANGES

TO:

Approved for public release; distribution is unlimited.

FROM:

**Distribution authorized to U.S. Gov't. agencies and their contractors;
Administrative/Operational Use; APR 1960. Other requests shall be referred to Air Force Air Research and Development Command, Arnold Engineering Development Center, Tullahoma, TN 37389.**

AUTHORITY

aedc ltr 18 may 1967

AEDC-TN-60-69

DETERMINATION OF OPTIMUM OPERATING PARAMETERS FOR THE 1-FOOT TRANSONIC TUNNEL UTILIZING CONE-CYLINDER BODIES OF REVOLUTION

By

William L. Chew, Jr.
PWT, ARO, Inc.

April 1960

ARNOLD ENGINEERING DEVELOPMENT CENTER
AIR RESEARCH AND DEVELOPMENT COMMAND
USAF

DETERMINATION OF OPTIMUM OPERATING PARAMETERS FOR THE 1-FOOT TRANSONIC TUNNEL UTILIZING CONE-CYLINDER BODIES OF REVOLUTION

By

William L. Chew, Jr.
PWT, ARO, Inc.

April 1960
ARO Project No. 210707
Contract No. AF 40(600)-800

CONTENTS

ILLUSTRATIONS

ABSTRACT

Tests were conducted in the 1-Foot Transonic Tunnel of the Propulsion Wind Tunnel Facility, AEDC, to determine optimum operating parameters which minimize tunnel interference effects with the 60-deg inclined hole, 6-percent open-area test section configuration. Pressure distributions on a 20-deg cone-cylinder model having a blockage ratio of 1.86 percent were used to determine optimum test section wall angle positions. A similar cone-cylinder model with 1-percent blockage ratio was used to investigate the effects of tunnel pressure ratio and support interference on base pressure measurements at various axial locations of the model in the test section.

Minimum tunnel interference on the pressure distribution of the 20-deg cone-cylinder model resulted by varying the wall angle from 40-min convergence to 30-min divergence for a Mach number range from 1.10 to 1.50. Below Mach number 1.10 the effect of varying wall angle on the pressure distribution was negligible. Base pressure coefficients on the 1-percent blockage model as affected by the axial position in the tunnel and variations in tunnel pressure ratios are presented.

NOMENCLATURE

$C_{p,b}$	Base pressure coefficient, $(p_b - p_\infty) / q_\infty$
d	Diameter of model base, in.
ℓ	Length, in.
M	Local Mach number
M_∞	Free-stream Mach number
p	Local static pressure, psf
p_b	Base pressure, psf
p_c	Plenum chamber static pressure, psf
p_t	Stilling chamber total pressure, psf
p_∞	Static pressure of undisturbed free stream, psf
q_∞	Dynamic pressure of undisturbed free stream, $0.7\, p_\infty\, M_\infty^2$, psf
x	Distance from model nose, in.
θ_w	Test section wall angle, minutes (positive when walls are diverged)
θ_w^*	Optimum test section wall angle, minutes
λ	Tunnel pressure ratio (ratio of tunnel total pressure to the static pressure downstream in the diffuser)

INTRODUCTION

The 1-Foot Transonic Tunnel of the Propulsion Wind Tunnel Facility, Arnold Engineering Development Center (PWT-AEDC) has been used extensively to develop a suitable test-section wall configuration for PWT's 16-Foot Transonic Circuit. The design of the wall liners was dictated primarily by the required ability to test full-scale propulsion units through the Mach number range from 0.50 to 1.60.

Typical full-scale propulsion units result in test-section blockage ratios appreciably larger than are normally considered desirable for transonic wind tunnels. Furthermore, the length of typical propulsion units relative to the height of the test section dictates that shock waves and expansions originating at the front end of the test article will affect the flow over the aft end of the test article through much of the low supersonic Mach number range if these disturbances are allowed to reflect from the tunnel walls. Reflected disturbances appeared to be a more severe problem than the subsonic blockage effects, and therefore, the primary criteria established for the test-section wall liners was the ability to cancel both compressions (shock waves) and expansions that impinge on the walls. A 20-deg cone-cylinder body was selected as a test model because it produces a compression field followed by a sharp expansion field. An extensive investigation was then made, primarily at a Mach number of 1.20, to find a wall geometry that would provide essentially interference-free pressure distributions over the test model at blockage ratios up to 2 percent.

As reported in Refs. 1 through 4, a perforated wall with a ratio of open area to closed area of 6 percent, and with the axes of the holes inclined 60 deg into the oncoming airstream, provided very good results. This wall geometry was adopted for both the 16-ft and 1-ft wind tunnels. Subsequent wall-interference studies (Ref. 5) have indicated that this wall geometry provides reasonably good interference characteristics at Mach numbers other than 1.20. However, the open area ratio with parallel walls is too large for optimum results at Mach numbers from 0.95 to 1.10 and too small at Mach numbers greater than 1.20. From the early studies it was discovered that the effective resistance to flow through perforated walls could be changed by varying the wall angle. This variation can be accomplished much more conveniently than varying the open-area ratio. Therefore, the first phase of the present investigation was undertaken to determine how much improvement in interference characteristics could be obtained by varying wall angle as a function of Mach number, to determine the optimum wall angle at each

---

Manuscript released by author March 1960.

Mach number, and to obtain calibration data at the optimum wall angle settings. As before, a 20-deg cone-cylinder body was used as a test model.

The object of the second phase of the investigation was to determine the maximum usable length of the test section of the 1-Foot Transonic Tunnel with the model support system and a typical sting adapter installed in the aft end of the test section. Data obtained from earlier calibrations have indicated that the Mach number distribution in the aft portion of the test section can be drastically affected by variations in tunnel pressure ratio (ratio of stilling-chamber total pressure to diffuser static pressure). This condition is particularly evident at subsonic speeds where the test section Mach number is a function of both the tunnel pressure ratio and the plenum suction rate. For each Mach number there is an optimum combination of the two variables which provides a constant Mach number throughout the length of the test section. If the tunnel pressure ratio is too high, the flow begins to accelerate in the aft portion of the test section. If the ratio is too low, pressure recovery will begin upstream in the test section.

This behavior has been investigated in the 1-Foot Transonic Tunnel with the model support strut removed and with pylon supported models to simulate propulsion tests in the 16-Foot Transonic Circuit (Ref. 6). The models were moved axially along the centerline of the test section, and the variation of base pressure with tunnel pressure ratio was determined at each model position for various Mach numbers. It is assumed that the base pressure is more sensitive to the effects in question than any other aerodynamic characteristic of a test body. The base pressure was independent of tunnel pressure ratio at the more forward locations but became increasingly sensitive to variations in tunnel pressure ratio as the model was moved aft. At each Mach number one value of tunnel pressure ratio was found to produce the same base pressure independent of model location. This pressure ratio was assumed to be optimum tunnel pressure ratio for that Mach number. This optimum value of tunnel pressure ratio was somewhat higher than the value which produced the most constant Mach number distribution without a model and indicated that the optimum tunnel pressure ratio is a function of model size or drag as would be expected.

This effect can be circumvented, however, by keeping the aft end of models upstream of the extreme aft end of the test section. When this is done the base pressure is independent of small changes in tunnel pressure ratio about the optimum value. An aft-most position can then be defined where the difference in optimum tunnel pressure ratio for models of maximum and minimum size is equal to or less than the increment of tunnel pressure ratios for which the base pressure is invariant. Then if the base of any model is kept upstream of this position and the

tunnel is operated at the optimum value of tunnel pressure ratio, the base pressure will be the same as if the test section were infinitely long.

The second phase of the present investigation involved an investigation of the relationship between model position and tunnel pressure ratio effects with a typical sting supported model mounted on the standard model support strut. The procedure used simultaneously provides data on support interference effects.

APPARATUS

1-FOOT TRANSONIC TUNNEL

The 1-Foot Transonic Tunnel is a continuous-flow, non-return wind tunnel. The tunnel is equipped with a two-dimensional flexible nozzle and a plenum evacuation system capable of establishing air speeds in the test section up to Mach number 1.50. A general arrangement of the tunnel components and supporting equipment is shown in Fig. 1. A more detailed description of the facility is presented in Ref. 7.

The test section consists of four perforated walls forming a test section 12 by 12 inches in cross-section and 37.5 inches in length. The top and bottom walls of the test section are supported by flexures at the nozzle exit and screw actuators at the downstream end to provide for wall angle adjustments. The side walls are not adjustable and are parallel. The perforated wall liners are 1/8-in. thick and have 1/8-in.-diam holes with the axes of the holes inclined into the airstream at an angle of 60 deg. The ratio of open to total area is 6 percent. A general arrangement of the test section and the geometry of the perforated wall is shown in Fig. 2. As indicated in Fig. 2, a linear variation in the distribution of the perforated openings extends from the nozzle exit to approximately 10 in. downstream to provide for smooth transition in the development of supersonic flow. This transition region was established by plugging the desired holes in the perforated wall (Fig. 3). Figure 3 also shows the axial probe used to determine the static pressure distribution along the centerline of the test section.

TEST ARTICLES

The data were primarily obtained from two models that were geometrically similar, each having a conical nose with a total included angle of 20 deg followed by constant-diameter cylindrical bodies. One model, which was used to obtain body pressure distribution data as a function of wall angle, has a cylinder diameter of 1.85 in. and a length

of 24 in. The ratio of model cross-sectional area to nozzle-exit area is 0.0186 (1.86-percent blockage) and the ratio of model length to diameter is 12.97. The model was instrumented with 45 static pressure orifices equally spaced along a meridian. The model was oriented along the tunnel centerline at zero angle of attack such that the apex of the cone was positioned at a station 12 in. from the nozzle exit. Figure 4 shows the model dimensions and a photograph of the model installation in the test section.

The second model, which was used to obtain base pressure measurements with the model at various stations along the centerline of the tunnel, has a cylinder diameter of 1.355 in. and a length of 8.82 in. The ratio of model cross-sectional area to nozzle-exit area is 0.01 (1-percent blockage) and the ratio of model length to diameter is 6.5. The model has an axisymmetrical hole which allows the model to mount on a 0.5-in.-diam probe as shown in Fig. 5. The probe was instrumented with 15 pressure orifices at 1 in. intervals and was mounted into an adapter supported by the model support system so that the last orifice was 0.5 in. forward of the adapter tip (station 32.2 in. downstream of the nozzle exit). The model could be moved along the probe to position the base of the model at each orifice. A seal was provided between the model and probe to prevent internal flow affecting base pressure measurements.

PROCEDURE

TUNNEL OPERATION

Subsonic and low supersonic Mach numbers through 1.10 were established in the test section with the sonic nozzle contour in conjunction with the proper combination of tunnel pressure ratio and plenum evacuation rate. Supersonic speeds were obtained with the flexible nozzle and with plenum suction to stablize the flow in the test section.

Condensation in the test section at supersonic speeds was prevented by raising the stagnation temperature. The stagnation temperature required varied with Mach number from 160 to 200°F. The average total pressure was approximately 2850 psfa.

Pressure distributions on the cone-cylinder model were obtained for variations in wall angle in 10-min increments at each Mach number from 1.00 to 1.50. The range of wall angles was varied for each Mach number. Since calibration data for each wall angle setting were not available, cone surface pressures were used as an indicator to establish the proper free-stream Mach number. Cone pressures were based on theoretical calculations and/or experimental data considered to be interference free. To

establish Mach number for each wall angle at a given stagnation pressure, the plenum evacuation rate was adjusted until the corresponding cone pressure was obtained.

To establish Mach number calibrations for the wall angle settings for which cone-cylinder pressure data were recorded, static pressures along the test section centerline were obtained with the probe shown in Fig. 3. Static pressures were also measured along the top perforated wall. These measurements were obtained for wall angle settings varying from -50 to +40 min in 10-min increments for Mach numbers from 0.60 to 1.50.

The finite probe (Fig. 5), without the model, was installed in the model support system adapter on the axial centerline of the test section. At each test Mach number, static pressures were measured along the probe and one of the perforated walls (all four walls parallel) for various tunnel pressure ratio settings. The 1-percent cone-cylinder model was installed on the probe such that the model base was located at the mid-point of a pressure orifice. The base of the model for this test was positioned at tunnel stations 24.7, 26.7, 28.7, and 30.7, while the probe support adapter was located at station 32.2. Base pressure measurements were obtained at various tunnel pressure ratios at each test Mach number and base position.

PRECISION OF MEASUREMENTS

An estimate of the precision of the measurements presented in this report is given in the following table:

ΔM	$\Delta\lambda$	$\Delta(p/p_t)$	$\Delta\theta_w$	$\Delta C_{p,b}$
±0.003	±0.002	±0.002	±2 min	±0.007

The precision in Mach number given above does not include the deviation from the mean value in the test region. This deviation is ±0.003 for Mach numbers up to 1.00 and is generally within ±0.007 for Mach numbers up to 1.50

RESULTS AND DISCUSSION

WALL ANGLE CALIBRATION

Pressure distributions along the cone-cylinder model as affected by varying the wall angle are presented in Fig. 6 for Mach numbers 0.80, 1.00, 1.10, 1.20, 1.30, 1.40, and 1.50. The solid curves in Figs. 6a, b, and c for Mach numbers 0.80, 1.00 and 1.10 are based on experimental

data considered to be interference free which were obtained from a similar model with a 0.008-percent blockage ratio in the 16-ft circuit. The solid curves for Mach numbers 1.20 through 1.50 are theoretical distributions based on calculations from Ref. 3.

Body pressure distributions on the cone-cylinder model at Mach number 0.80 are presented in Fig. 6a. It is concluded from these data that the pressure distributions at subsonic speeds are unaffected by moderate wall angle variations. At Mach number 1.00 (Fig. 6b) it is apparent that the interference on the body pressure distribution is unaffected by changes in wall angle. This would be expected since results in Ref. 5 showed that this interference effect existed even when the wall open-area ratio was reduced to 1 1/2-percent. At Mach number 1.10 and with the walls parallel (Fig. 6c), a similar interference was evident. By converging the walls to - 40 min, the strength of the disturbance and the region over which it affected the body pressure distribution were reduced but not completely eliminated. At Mach number 1.20 (Fig. 6d), the data indicate that minimum wall interference effects occur when the walls are nearly parallel. For Mach numbers 1.30, 1.40, and 1.50 (Figs. 6e, f, and g, respectively) the pressure distributions show that a slight increase (divergence) in the wall angle was required to minimize the interference effects.

Pressure distributions on the 20-deg cone-cylinder model for each optimum wall angle position for Mach numbers from 0.60 to 1.50 are presented in Fig. 7. For test section Mach numbers of 1.00 and below the effects of varying the wall angle on the body pressure distributions are negligible. Thus, a parallel wall setting is used to simplify and speed operations. For Mach numbers above 1.00 the wall angle requirement varies from - 40 min at Mach number 1.10 to + 30 min at Mach number 1.50. Figure 8 presents the optimum test section wall angle as a function of Mach numbers.

MACH NUMBER CALIBRATION

Mach number distributions determined from static pressures measured along the tunnel centerline and along one perforated wall without a model in the test section are presented in Fig. 9 for the various wall angles investigated during the interference evaluation. Mach number distributions determined from static pressures measured on the perforated wall are normally used for reference only. The data in Fig. 9 indicate that the deviation in Mach number from a mean value in the usable test region is within ± 0.003 for Mach numbers up to 1.00. The Mach number deviation in the range above 1.00 is generally within ± 0.007. The tunnel pressure ratio for each free-stream Mach number was adjusted to maintain a constant Mach number distribution near the exit of the test

section. The corresponding pressure ratio for each Mach number is included in Fig. 9. It should be pointed out that although the flow near the exit of the test section is altered by variations in tunnel pressure ratio, the up-stream test section Mach number is not affected as long as the reference plenum chamber pressure is maintained at the proper value.

The plenum chamber pressure, p_c, is used as a reference pressure to set and calculate the average free-stream Mach number in the test section. The difference between the free-stream and plenum static pressure ratios is normally used as a calibration factor for calculating free-stream Mach number. This factor, $(p_\infty - p_c)/p_t$, is presented as a function of Mach number in Fig. 10 for the various wall angles at which data were obtained.

PRESSURE RATIO AND SUPPORT INTERFERENCE EFFECTS

The effects of variations in tunnel pressure ratio on the Mach number distribution in the aft portion of the test section (parallel walls) with the adapter and probe installed (without model) are presented in Fig. 11. The adapter probe combination is representative of the support configuration for many sting supported test models. The distributions along the perforated wall and the centerline probe at each free-stream Mach number are presented in Fig. 11. At subsonic speeds (Fig. 11a), the probe readings indicated a strong pressure rise immediately upstream of the adapter for all pressure ratios tested. The pressure rise is the result of interference of the adapter on the flow field with its influence extending to the wall pressures. For speeds above Mach number 1.00 (Figs. 11b and c) the distributions near the rear of the test section are unaffected by variations in the tunnel pressure ratios for the range of pressure ratios investigated. This would be expected since the pressure ratio was not reduced sufficiently to allow the shock to move from the diffuser into the downstream portion of the test section, which generally results in a rapid increase in plenum flow rate and unstable flow conditions. The compression effects on the wall and probe at the rear of the test section (Figs. 11b and c) are also a result of adapter interference on the flow field which diminishes with increasing free-stream Mach number.

The effects of varying tunnel pressure ratio on base pressure coefficients for several model base positions are presented in Fig. 12. For the conditions shown in Fig. 12a, the tunnel pressure ratio required to establish Mach number 0.70 was approximately 1.10. At this pressure ratio, the base pressure coefficients were of the same order of magnitude when the model base was 2.6 base diameters, or greater, forward of the adapter. When the model base was moved rearward toward the adapter, a reduction in base pressure coefficient as a

result of adapter interference was evident. An increase in tunnel pressure ratio greater than approximately 1.1 results in an increase in the free-stream Mach number. The data at Mach numbers 0.80 and above (Figs. 12a, b, and c) indicate that for each model base position, base pressure coefficients are only slightly affected by variations in tunnel pressure ratio for the range of pressure ratio investigated. More important in Fig. 12 is the change in the magnitude of the base pressure coefficient as the model is moved downstream. The data in Fig. 12 have been cross-plotted and presented in Fig. 13 to show the variation in base pressure coefficient as a function of model base position for various values of tunnel pressure ratio. It is clearly seen from Fig. 13 that as the model base position is moved rearward in the test section, the predominant factor affecting base pressure coefficient is support interference. The data of Fig. 13 show that if the model base is positioned no further rearward than station 26.7, base pressure coefficients are unaffected by support interference for Mach numbers from 0.7 to 1.50. The results in Fig. 13 also indicate that the effect of varying tunnel pressure ratio on base pressure coefficients is not serious, particularly if the model base is sufficiently forward to avoid support interference effects.

The results presented are for only one configuration which represents a typical installation. However, for other configurations which are not comparable, consideration must be given to other parameters such as model base shape and size, the ratio of model base diameter to sting diameter, and the included angle of the adapter.

CONCLUSIONS

This investigation to provide optimum operating parameters for the 1-Foot Transonic Tunnel utilizing 20-deg cone-cylinder bodies of revolution has resulted in the following conclusions:

1. Body pressure distributions on the 20-deg cone-cylinder body of revolution are unaffected by moderate wall angle variations at subsonic speeds.
2. Tunnel boundary interference on the 20-deg cone-cylinder pressure distributions in the Mach number range from 0.95 to 1.10 cannot be eliminated entirely with this wall configuration.
3. To minimize wall boundary interference on pressure distributions on the 20-deg cone-cylinder body of revolution at supersonic speeds requires varying the test section wall angle with Mach number, ranging from -40 min (convergence) at Mach number 1.10 to +30 min (divergence) at Mach number 1.50.

4. The predominant factor affecting base pressure coefficients is support interference. For the model configuration investigated, station 26.7 is the most rearward base position where base pressure coefficients are unaffected by support interference for all Mach numbers investigated.

5. Base pressure coefficients are not seriously affected by variations in tunnel pressure ratio, particularly if the model base is positioned sufficiently forward to avoid support interference.

REFERENCES

1. Goethert, B. H. "Physical Aspects of Three-Dimensional Wave Reflections in Transonic Wind Tunnels at Mach Number 1.20 (Perforated, Slotted, and Combined Slotted-Perforated Walls)." AEDC-TR-55-45, March 1956.

2. Gray, J. Don and Gardenier, Hugh E. "Experimental and Theoretical Studies on Three-Dimensional Wave Reflection in Transonic Test Sections, Part I: Wind-Tunnel Tests on Wall Interference of Axisymmetric Bodies at Transonic Mach Numbers." AEDC-TN-55-42, March 1956.

3. Dubose, H. C. "Experimental and Theoretical Studies on Three-Dimensional Wave Reflection in Transonic Test Sections, Part II: Theoretical Investigation of the Supersonic Flow Field about a Two-Dimensional Body and Several Three-Dimensional Bodies at Zero Angle of Attack." AEDC-TN-55-43, March 1956.

4. Chew, W. L. "Experimental and Theoretical Studies on Three-Dimensional Wave Reflection in Transonic Test Sections, Part III: Characteristics of Perforated Test-Section Walls with Differential Resistance to Cross-Flow." AEDC-TN-55-44, March 1956.

5. Estabrooks, Bruce B. "Wall-Interference Effects on Axisymmetric Bodies in Transonic Wind Tunnels with Perforated Wall Test Sections." AEDC-TR-59-12, June 1959.

6. Rittenhouse, L. E. "Base Pressure Effects Resulting from Changes in Tunnel Pressure Ratio in a Transonic Wind Tunnel." AEDC-TN-58-88, January 1959.

7. Test Facilities Handbook, (2nd Edition). "Propulsion Wind Tunnel Facility, Vol. 3." Arnold Engineering Development Center, January 1959.

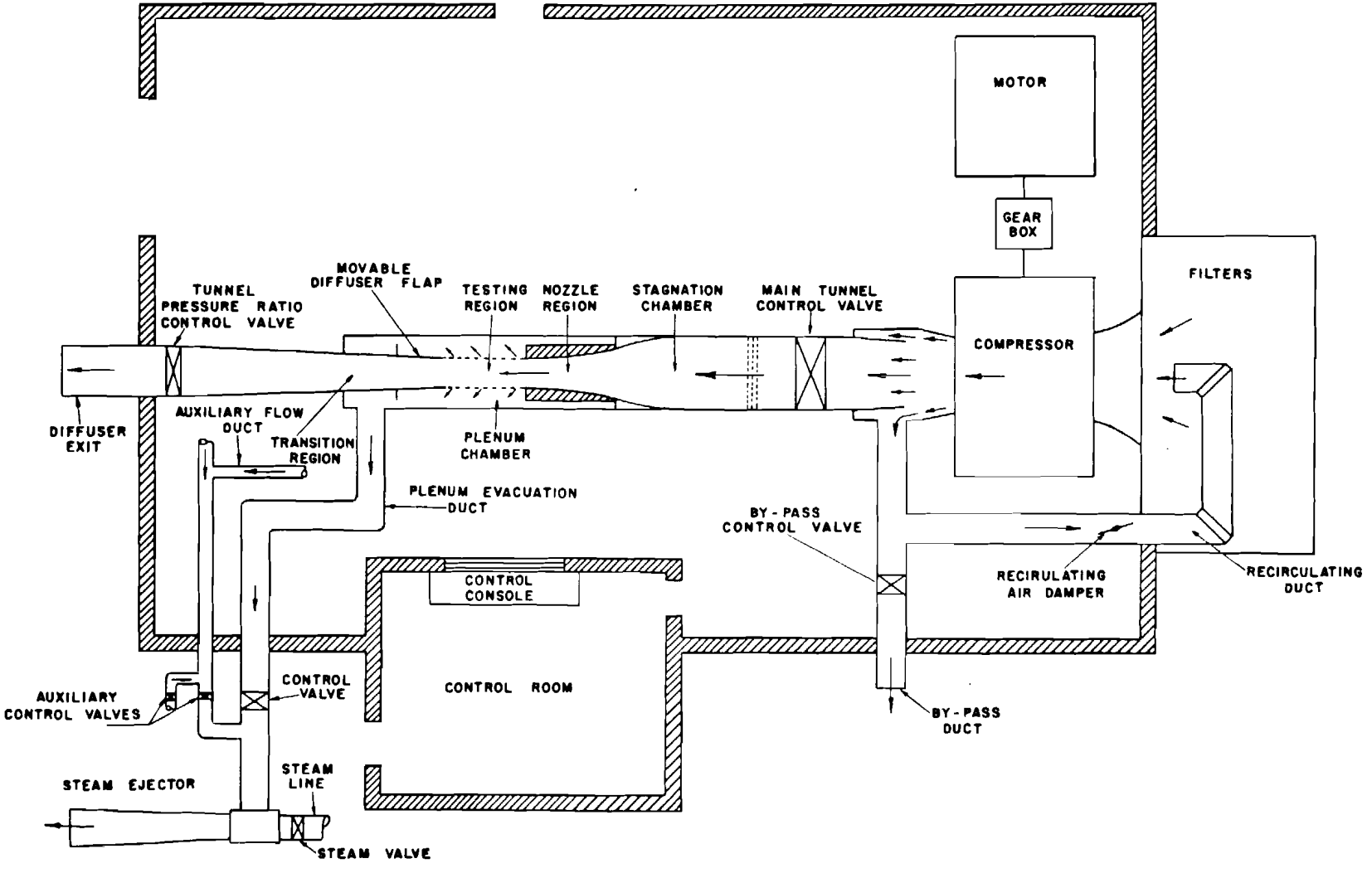

Fig. 1 General Arrangement of the 1-Foot Transonic Tunnel and Supporting Equipment

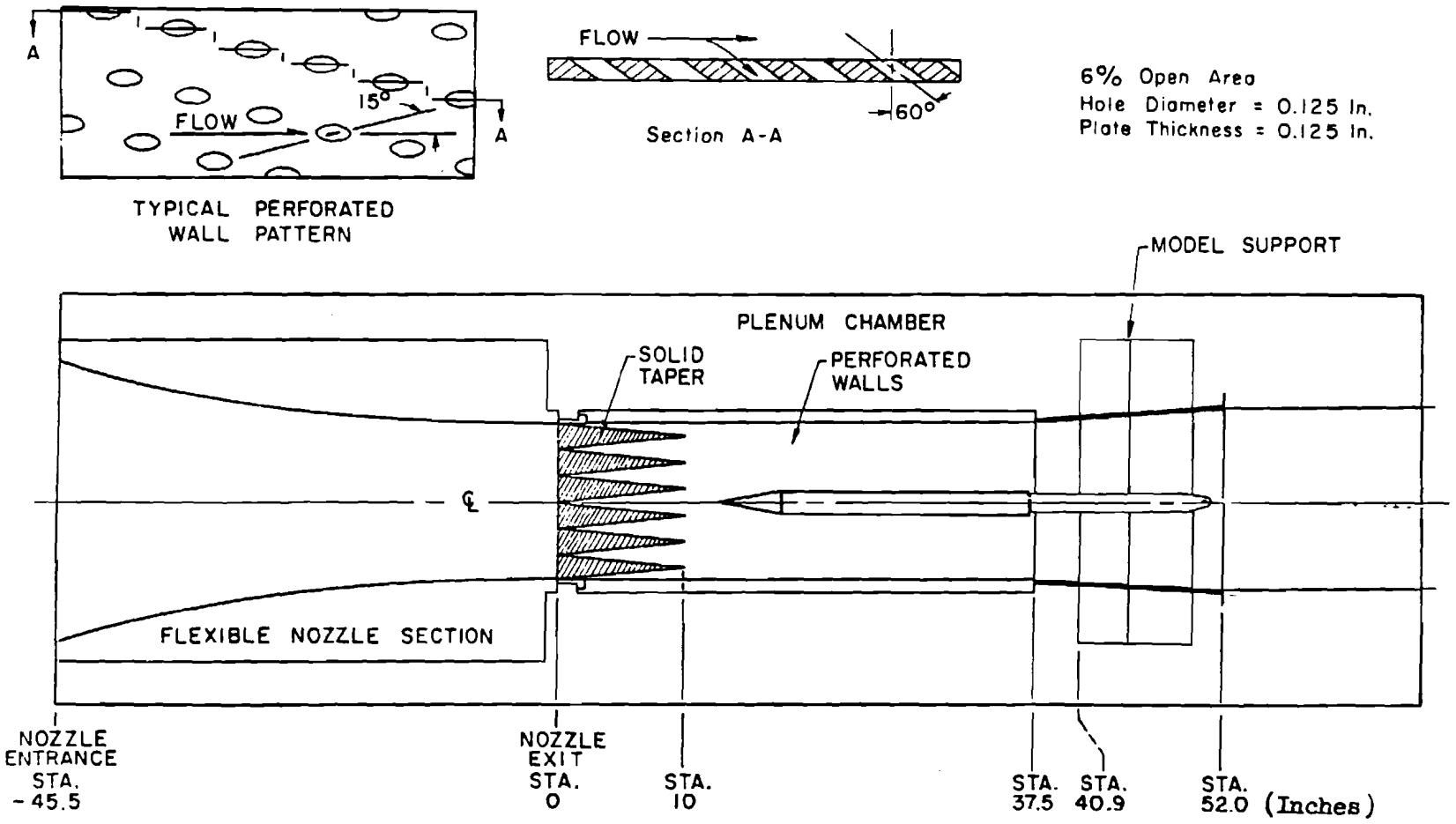

Fig. 2 Installation of Model Support in 1-Foot Transonic Tunnel

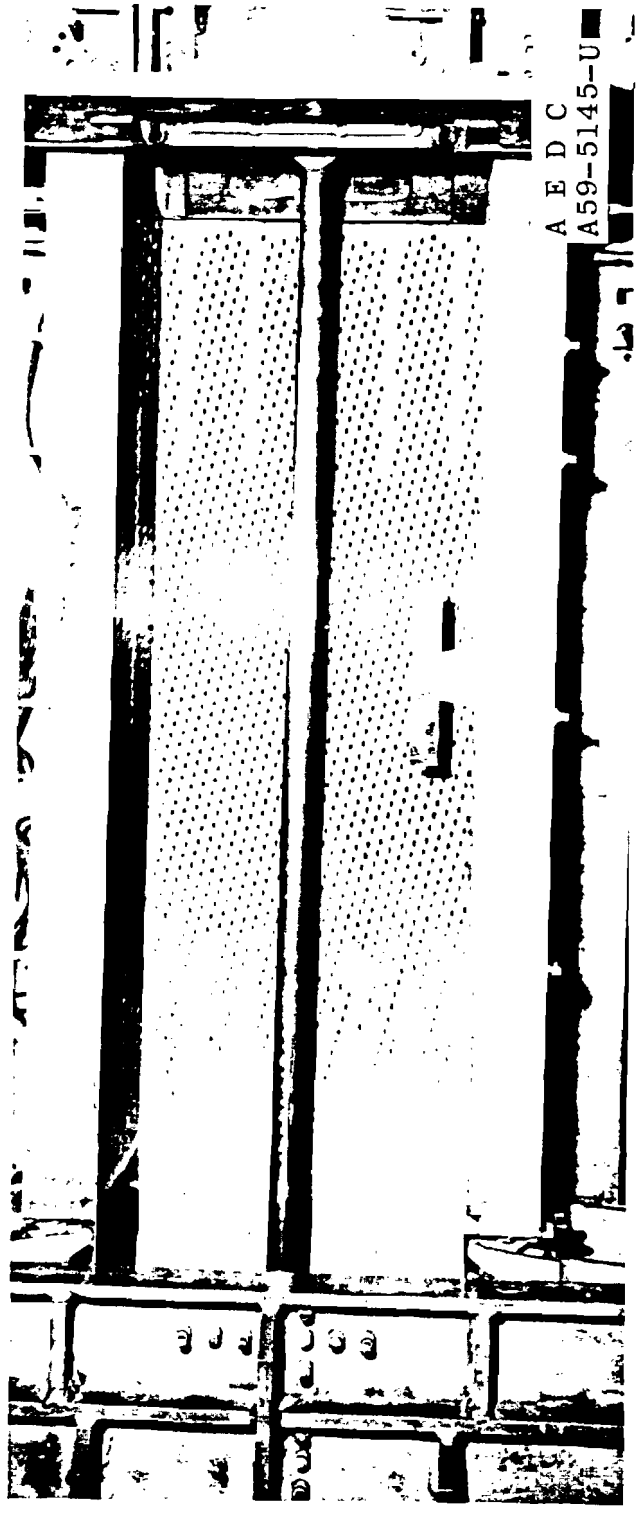

Fig. 3 Calibration Probe Installed in 1-Foot Transonic Tunnel Test Section Region

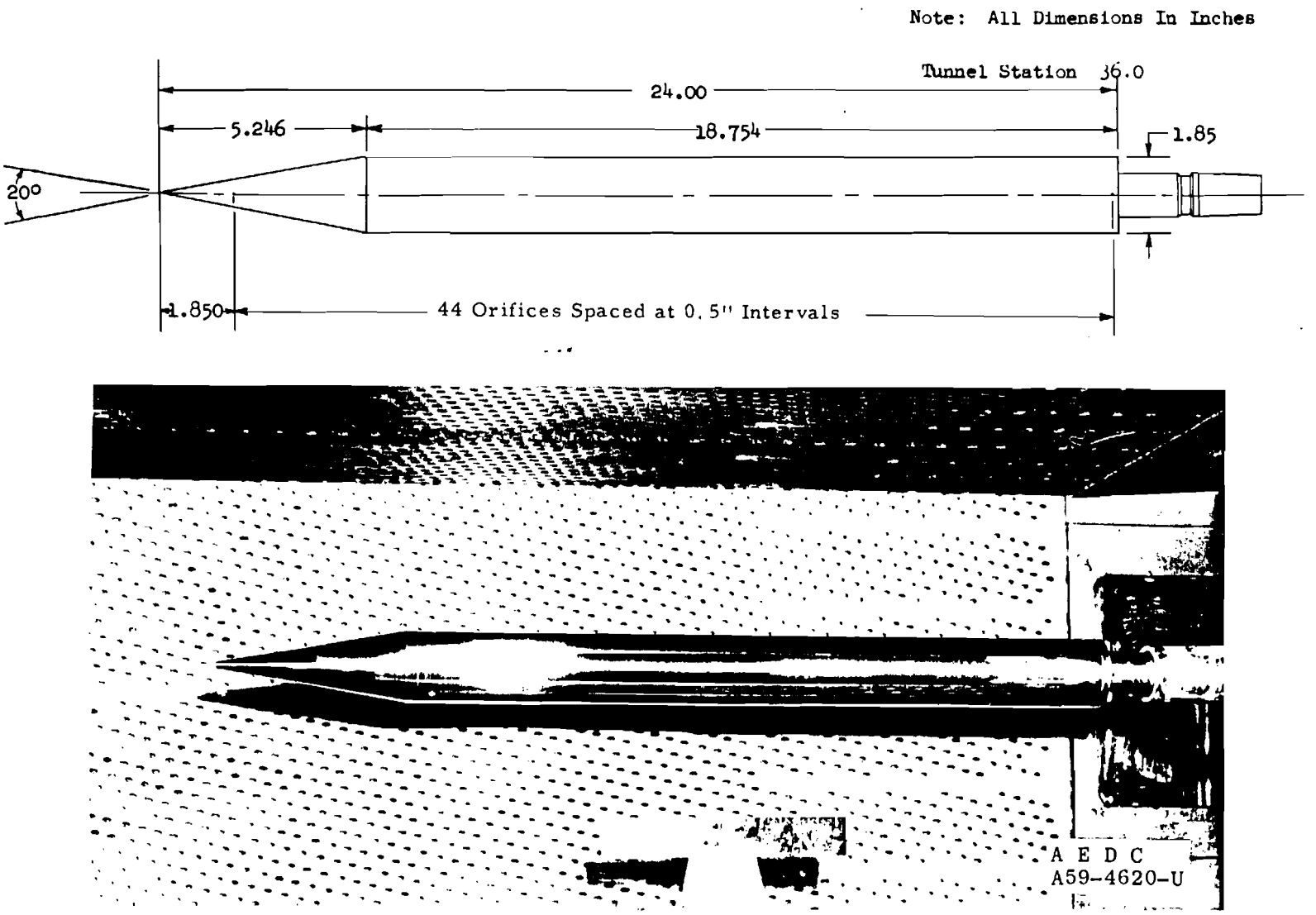

Fig. 4 A 20° Cone-Cylinder Model (1.86-Percent Blockage Ratio) Installed in the 1-Foot Transonic Tunnel

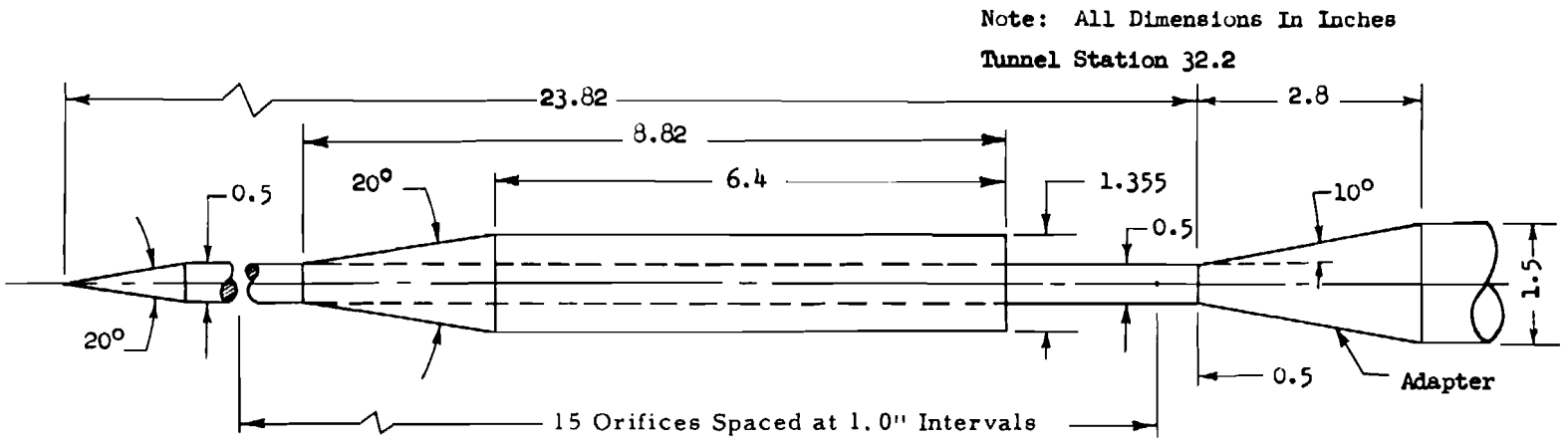

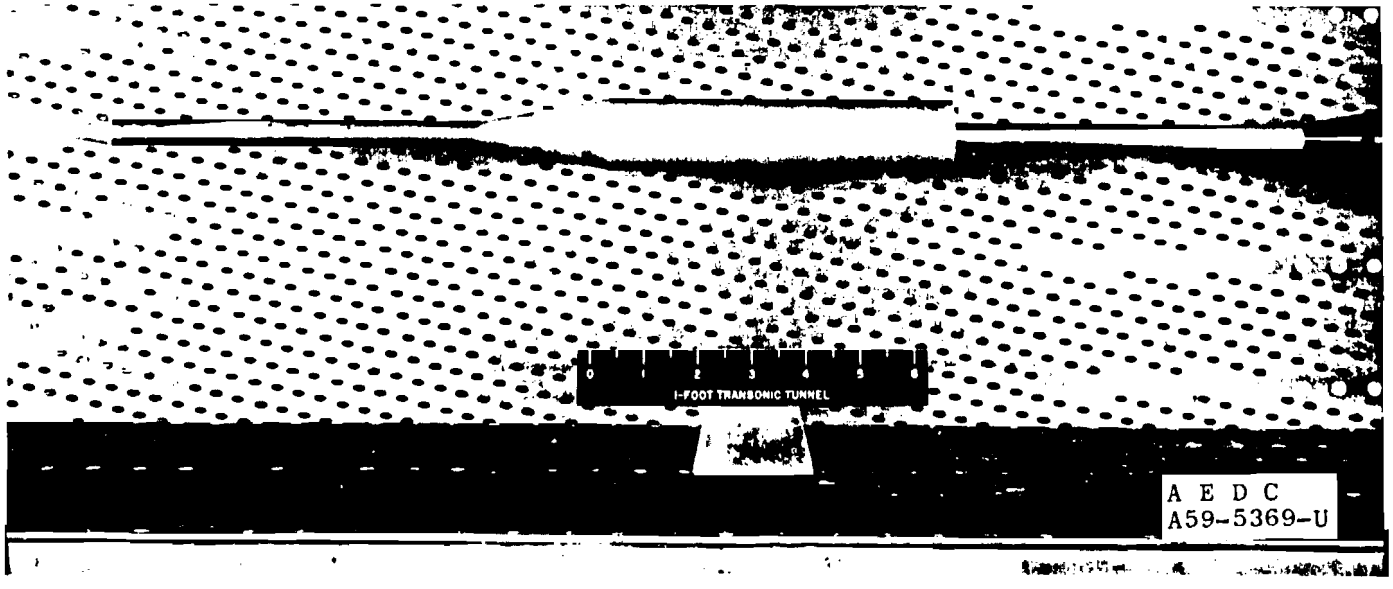

Fig. 5 Pressure Ratio Calibration Model Installed in 1-Foot Transonic Tunnel

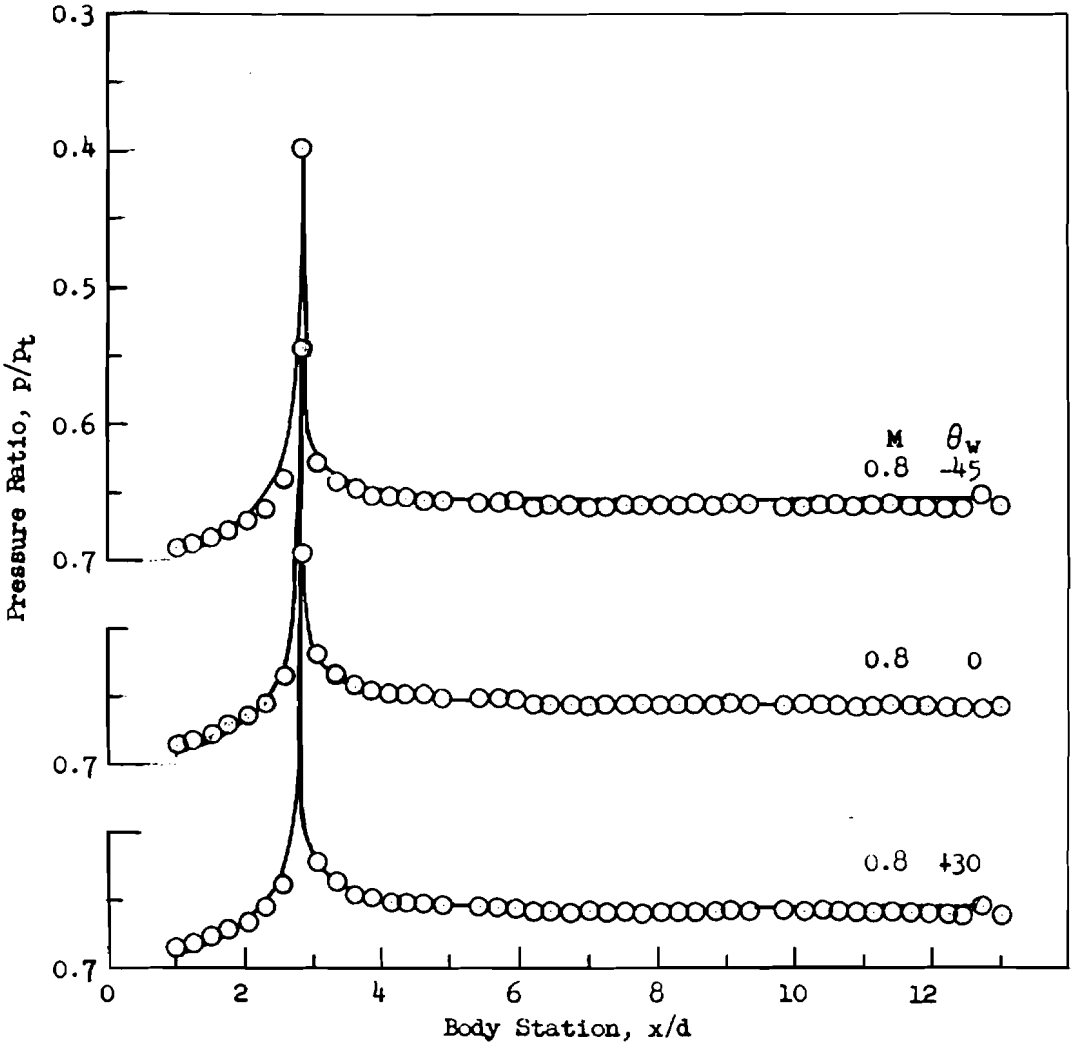

a. $M_\infty = 0.80$

Fig. 6 Body Pressure Distributions on the 1.86-Percent, 20° Cone-Cylinder Model; Effect of Wall Angle Variations with 60° Inclined-Hole, 6-Percent Open-Area Ratio Walls

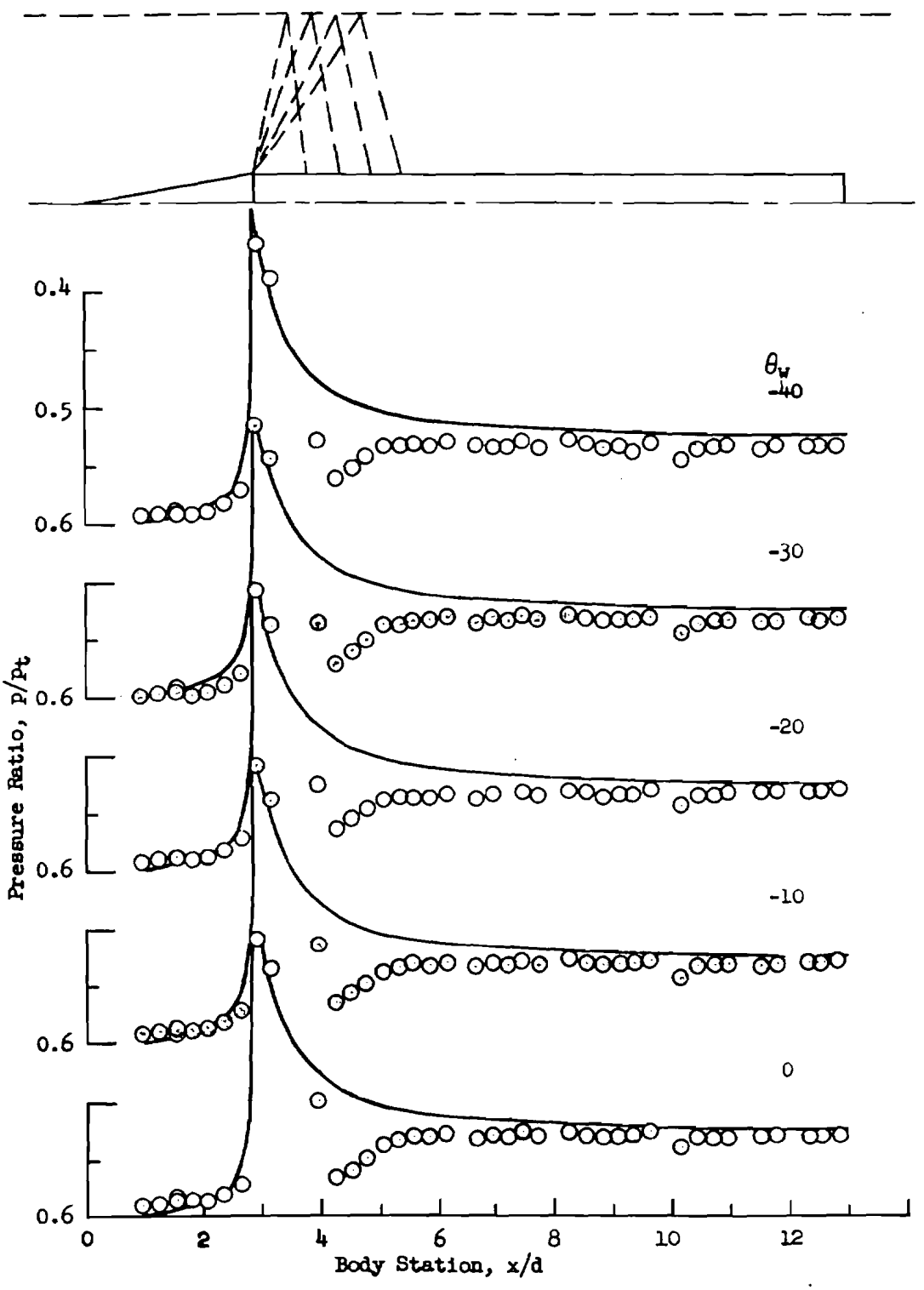

b. $M_\infty = 1.00$

Fig. 6 Continued

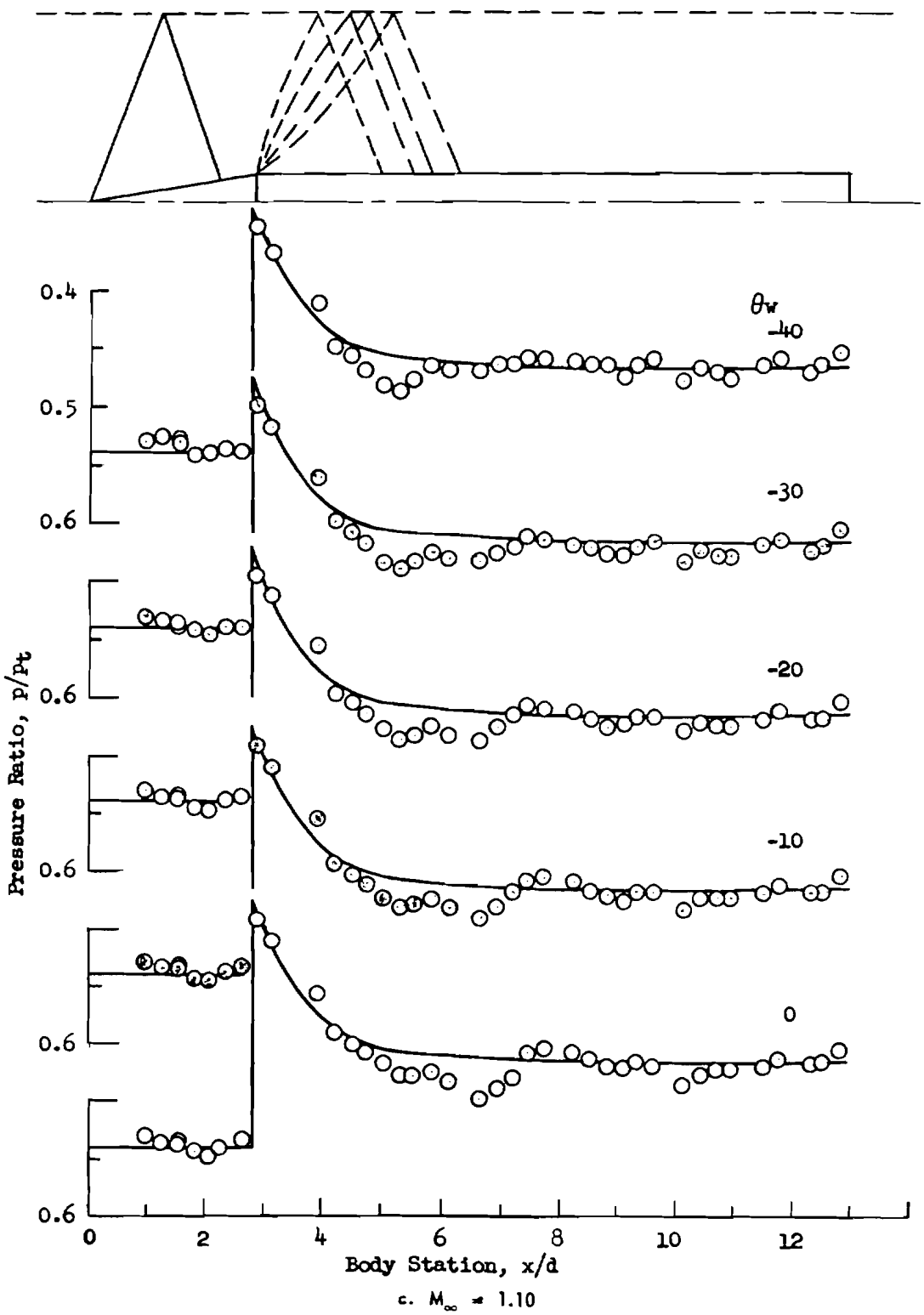

c. $M_\infty = 1.10$

Fig. 6 Continued

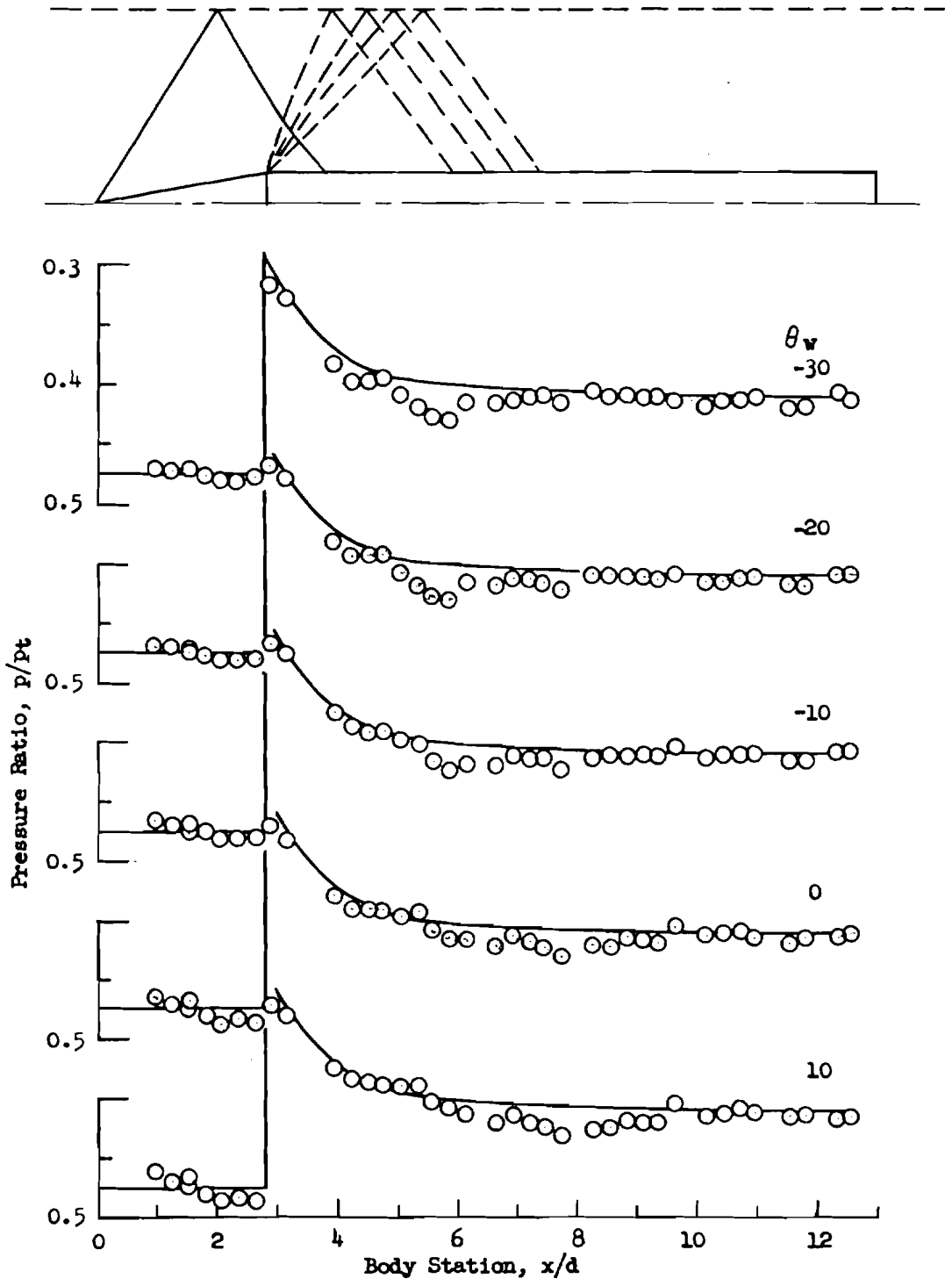

d. M_∞ = 1.20

Fig. 6 Continued

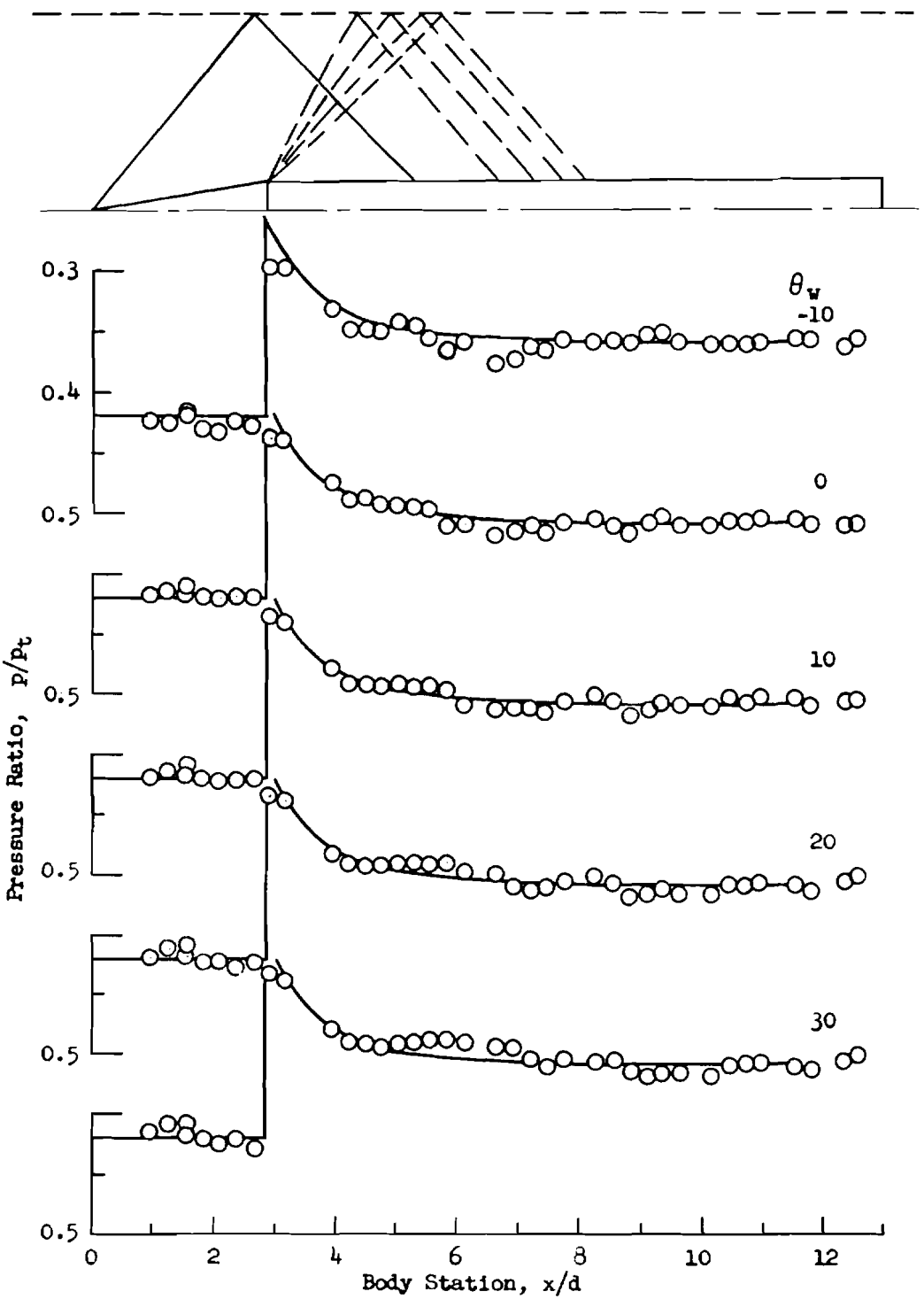

e. $M_\infty = 1.30$

Fig. 6 Continued

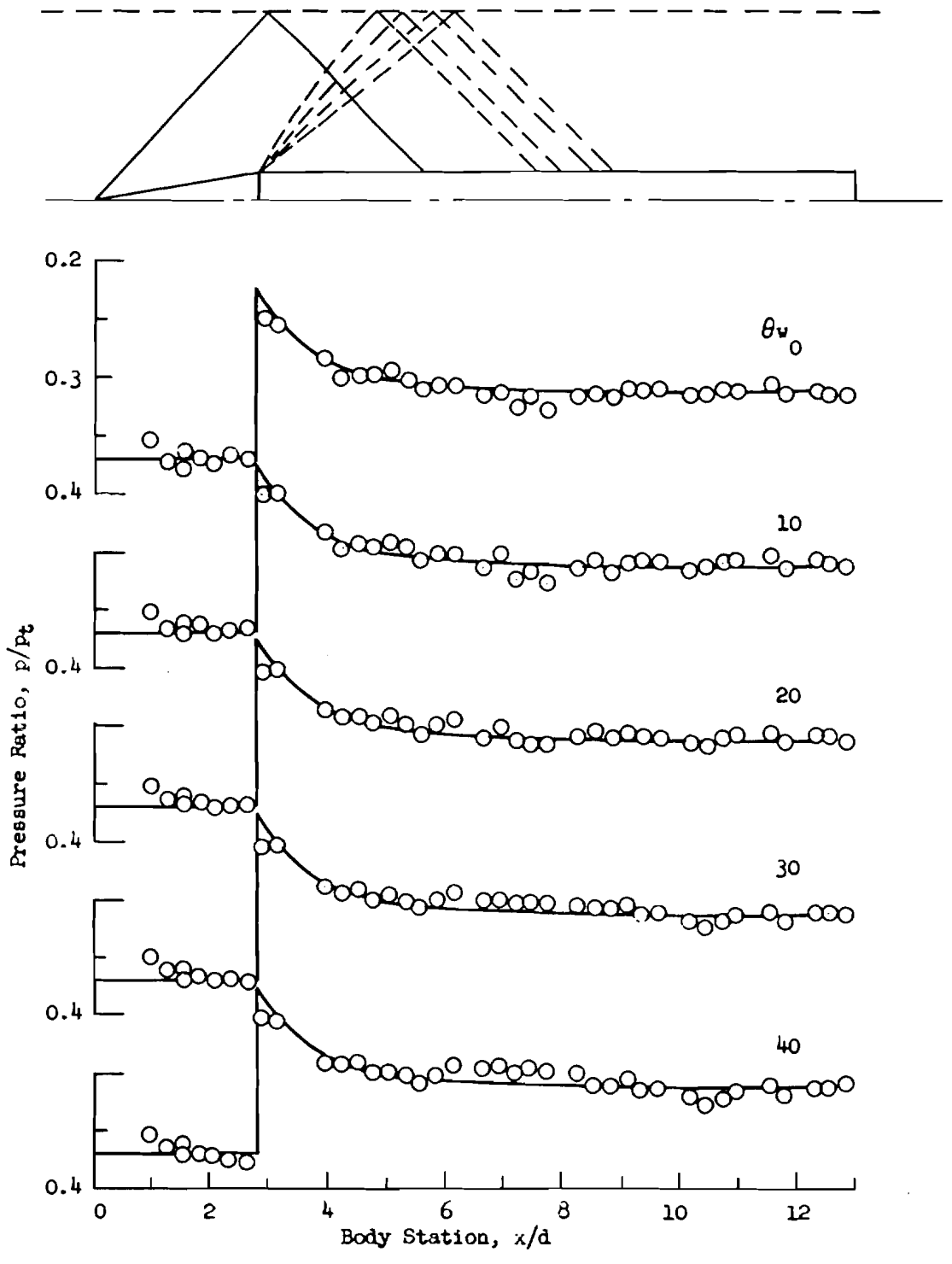

f. M_∞ = 1.40

Fig. 6 Continued

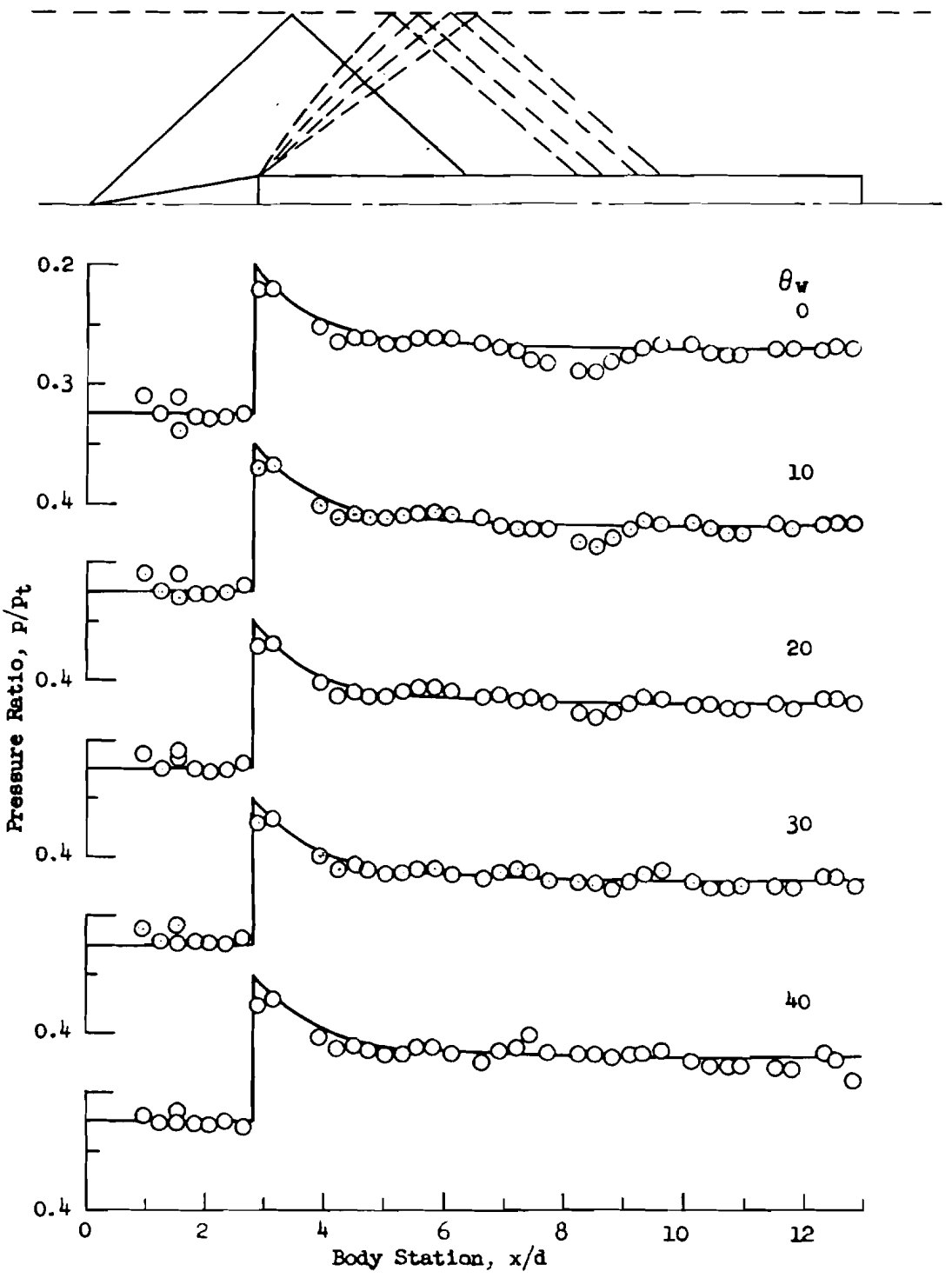

g. M_{∞} = 1.50

Fig. 6 Concluded

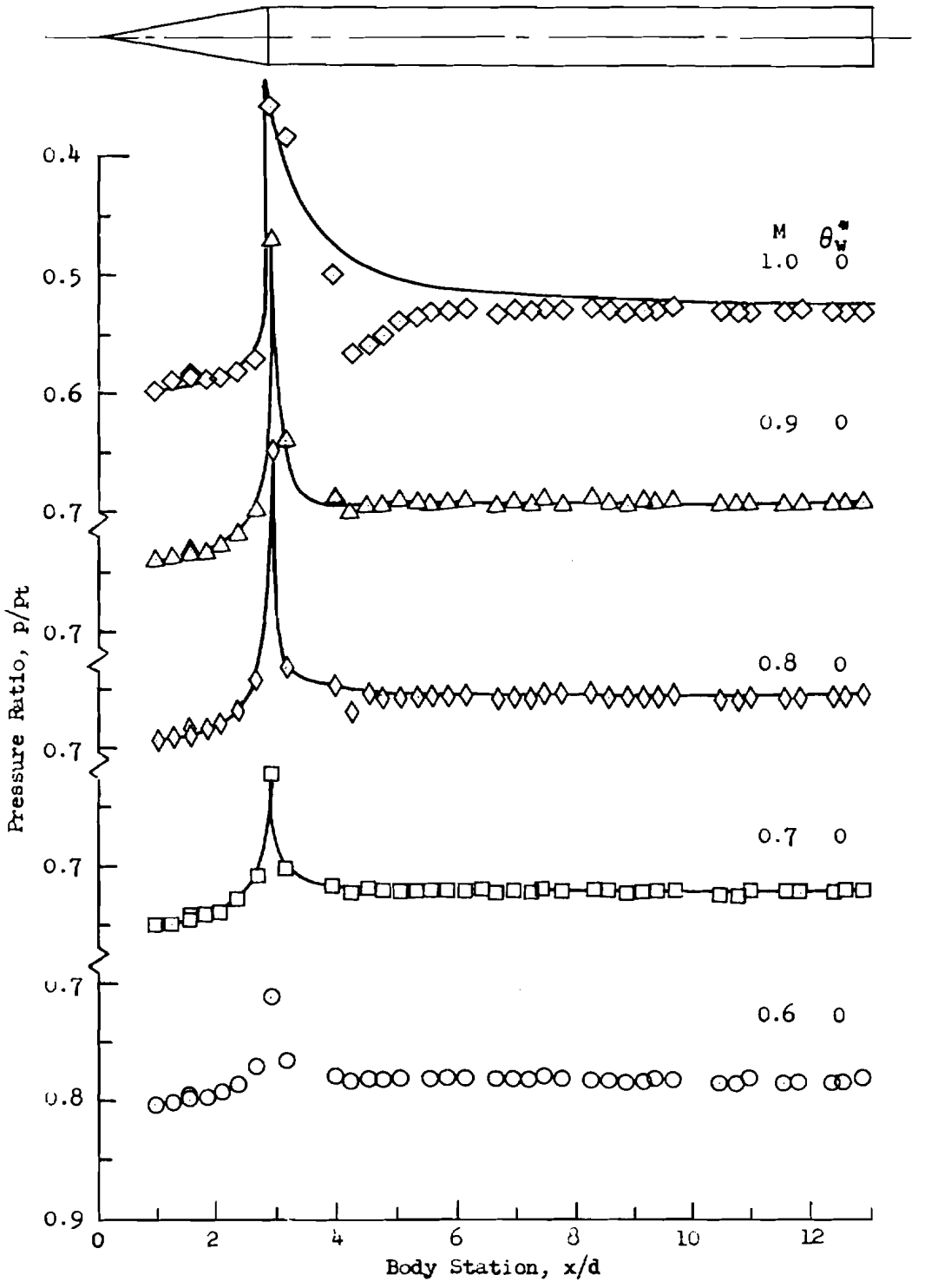

a. M_∞ = 0.60, 0.70, 0.80, 0.90, and 1.00

Fig. 7 Body Pressure Distributions on the 20° Cone-Cylinder Model for Each Optimum Wall Angle Position for the 60° Inclined-Hole, 6-Percent Open-Area Ratio Walls

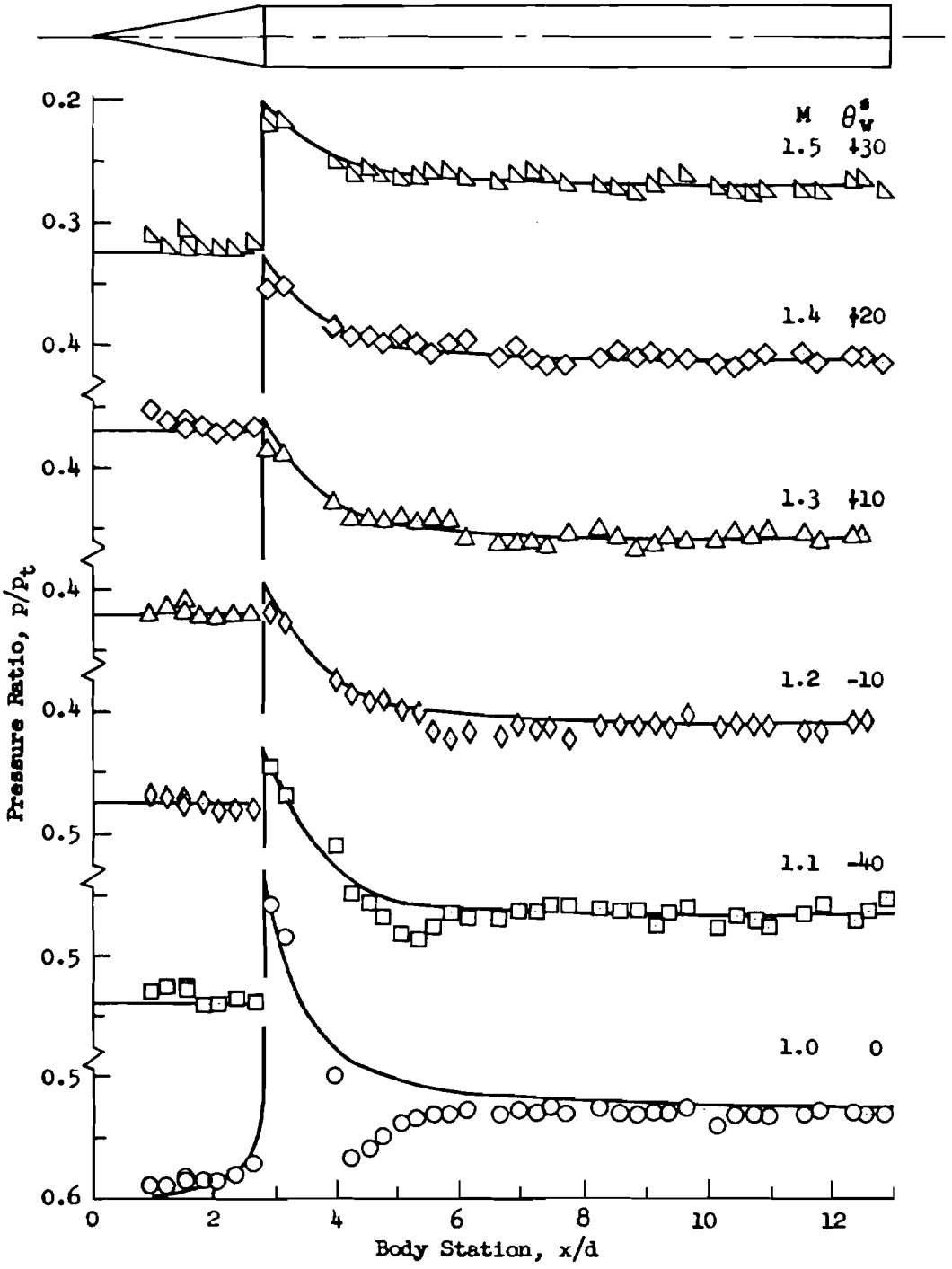

b. M_∞ = 1.00, 1.10, 1.20, 1.30, 1.40, and 1.50

Fig. 7 Concluded

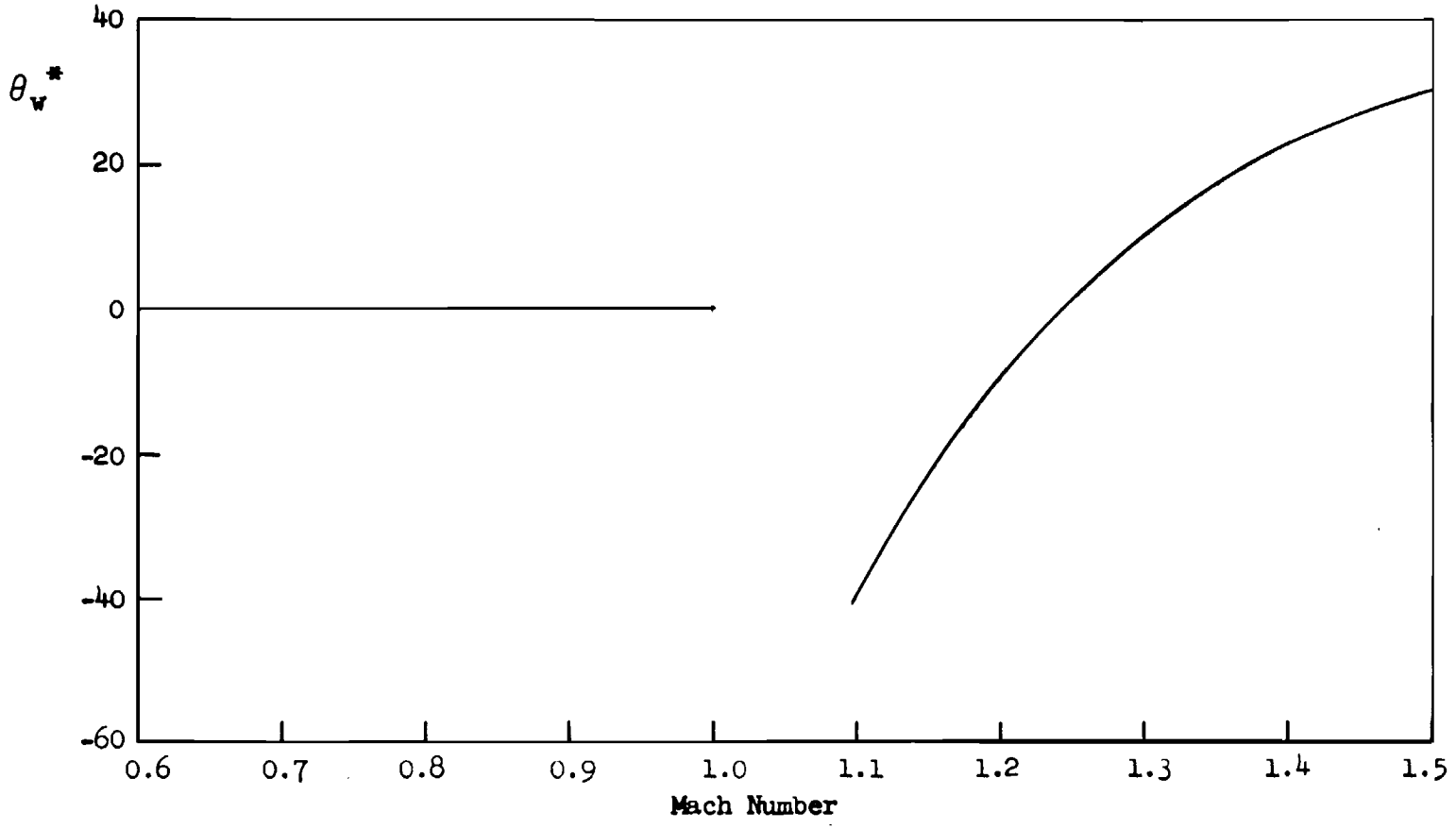

Fig. 8 Variation of Optimum Test Section Wall Angles, θ_w^*, with Mach Number

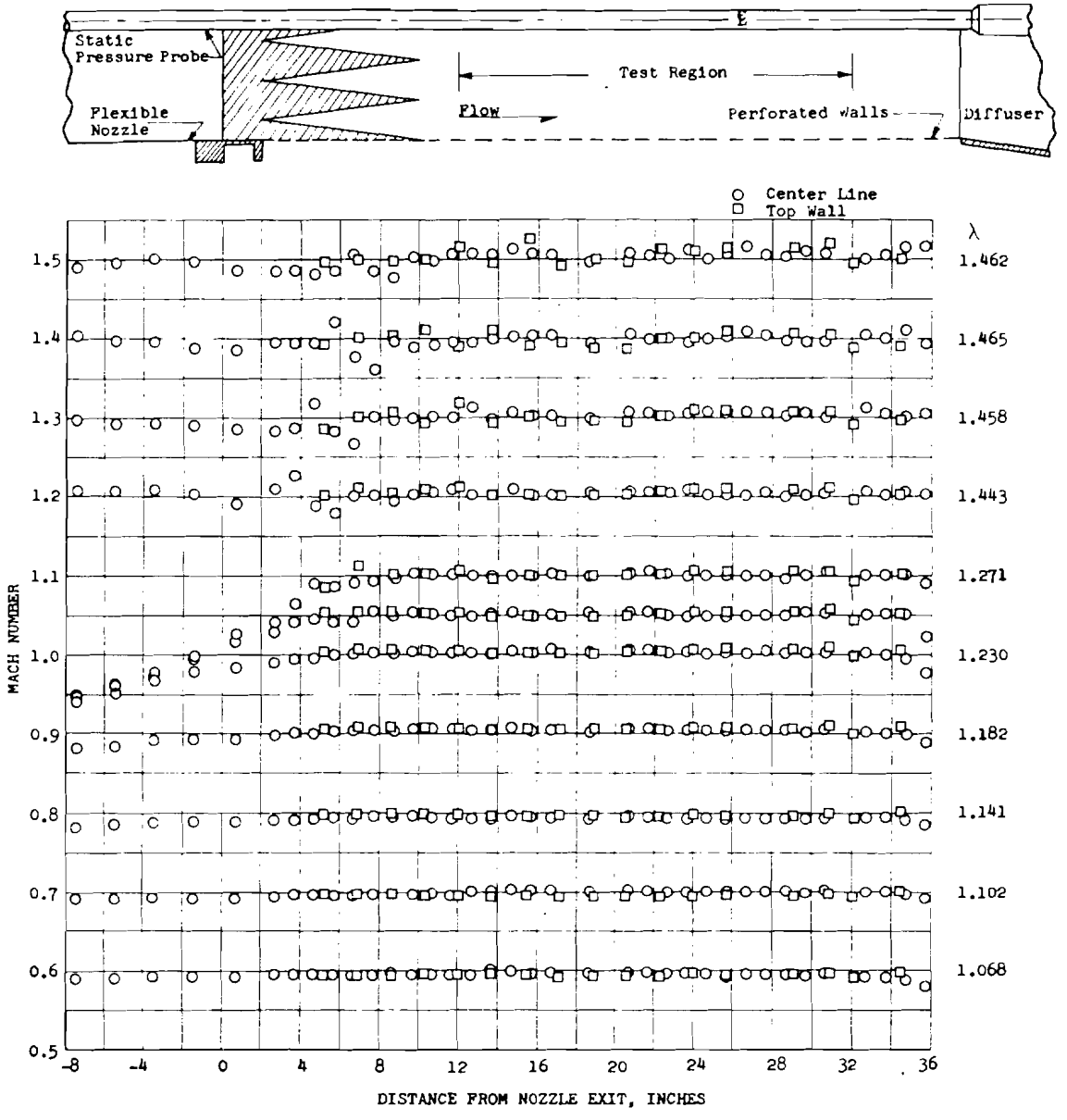

a. θ_w = 0 min

Fig. 9 Effect of Wall Angle Variations on the Test Section Mach Number Distribution

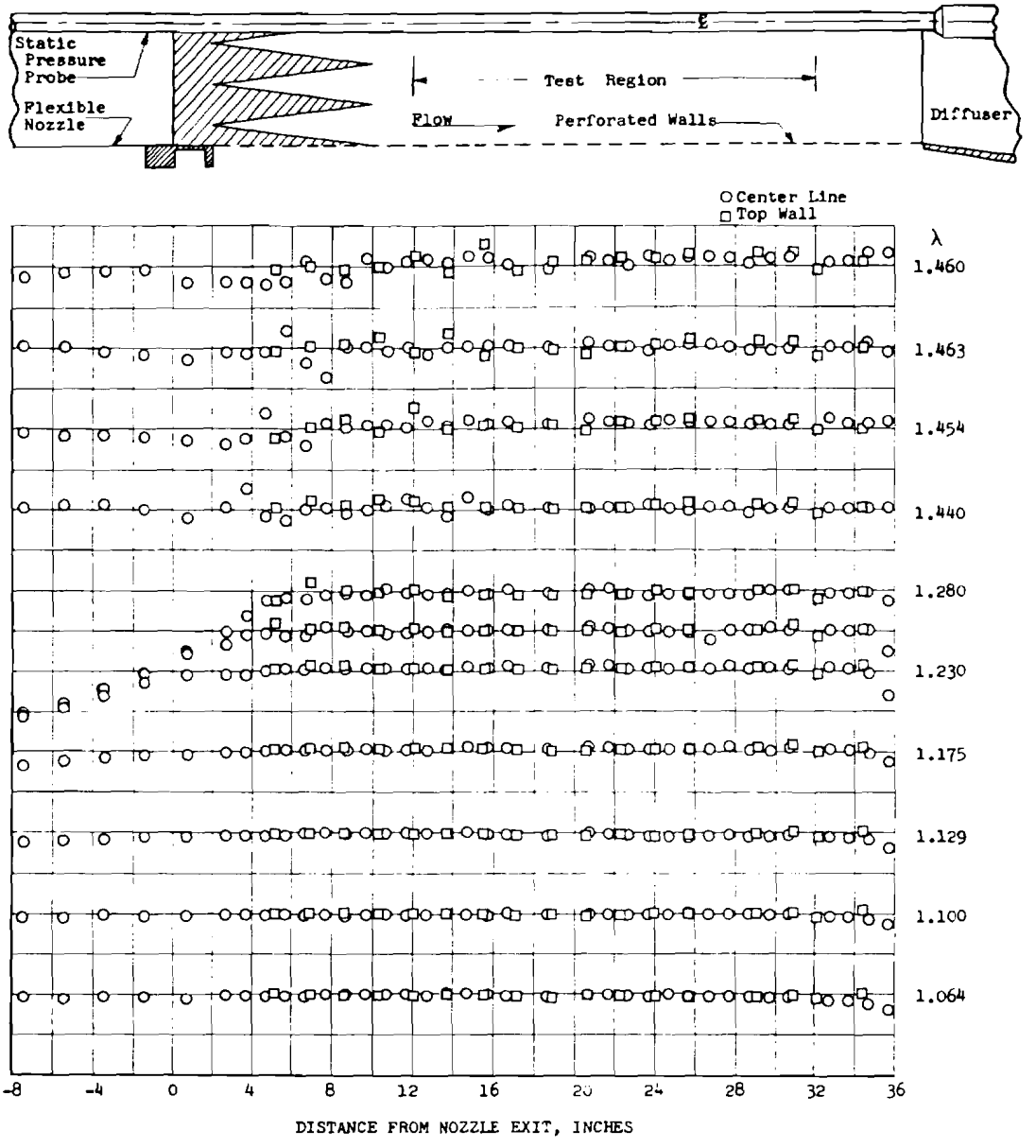

b. θ_w = + 10 min

Fig. 9 Continued

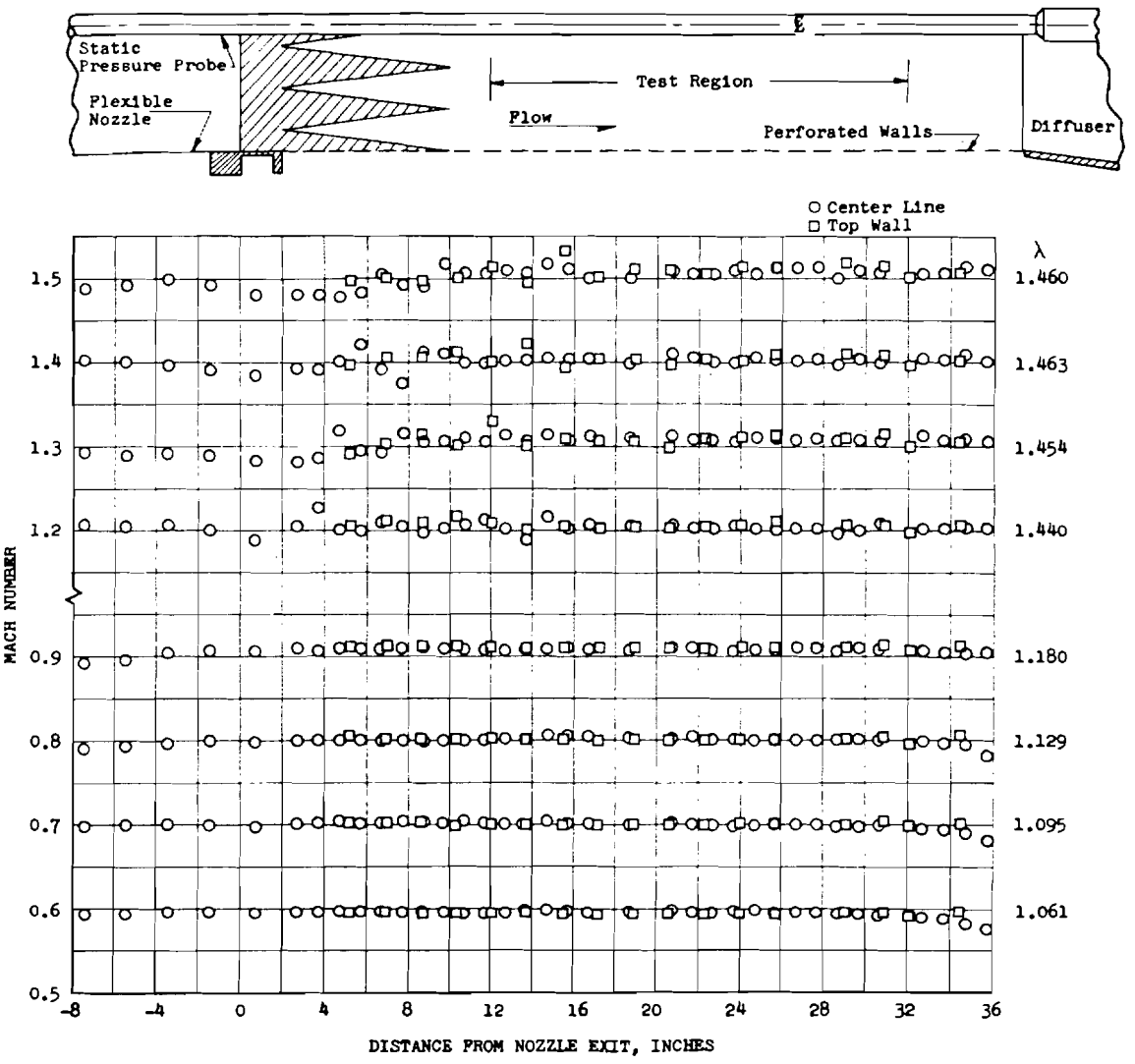

c. θ_w = + 20 min

Fig. 9 Continued

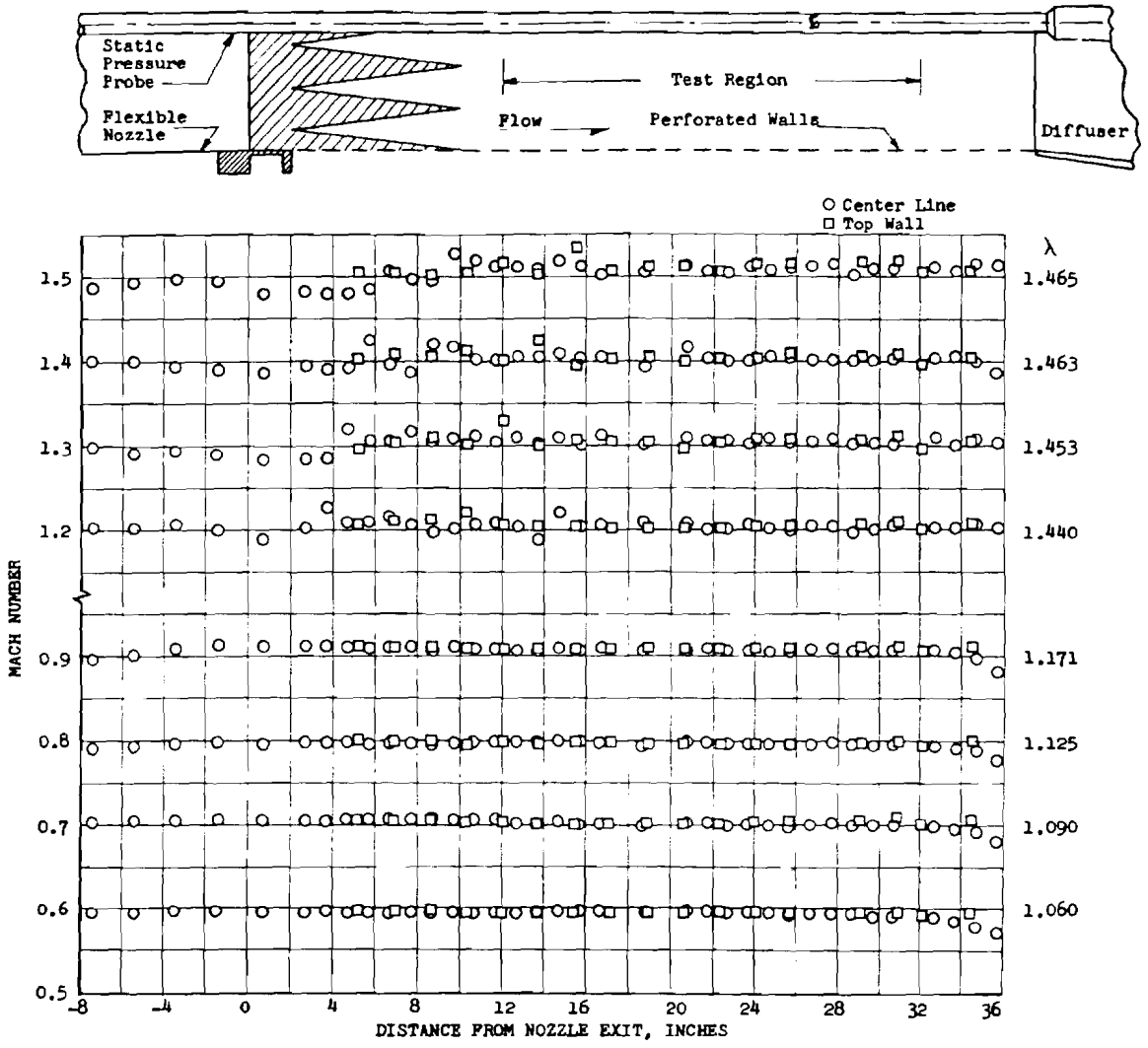

d. θ_w = +30 min

Fig. 9 Continued

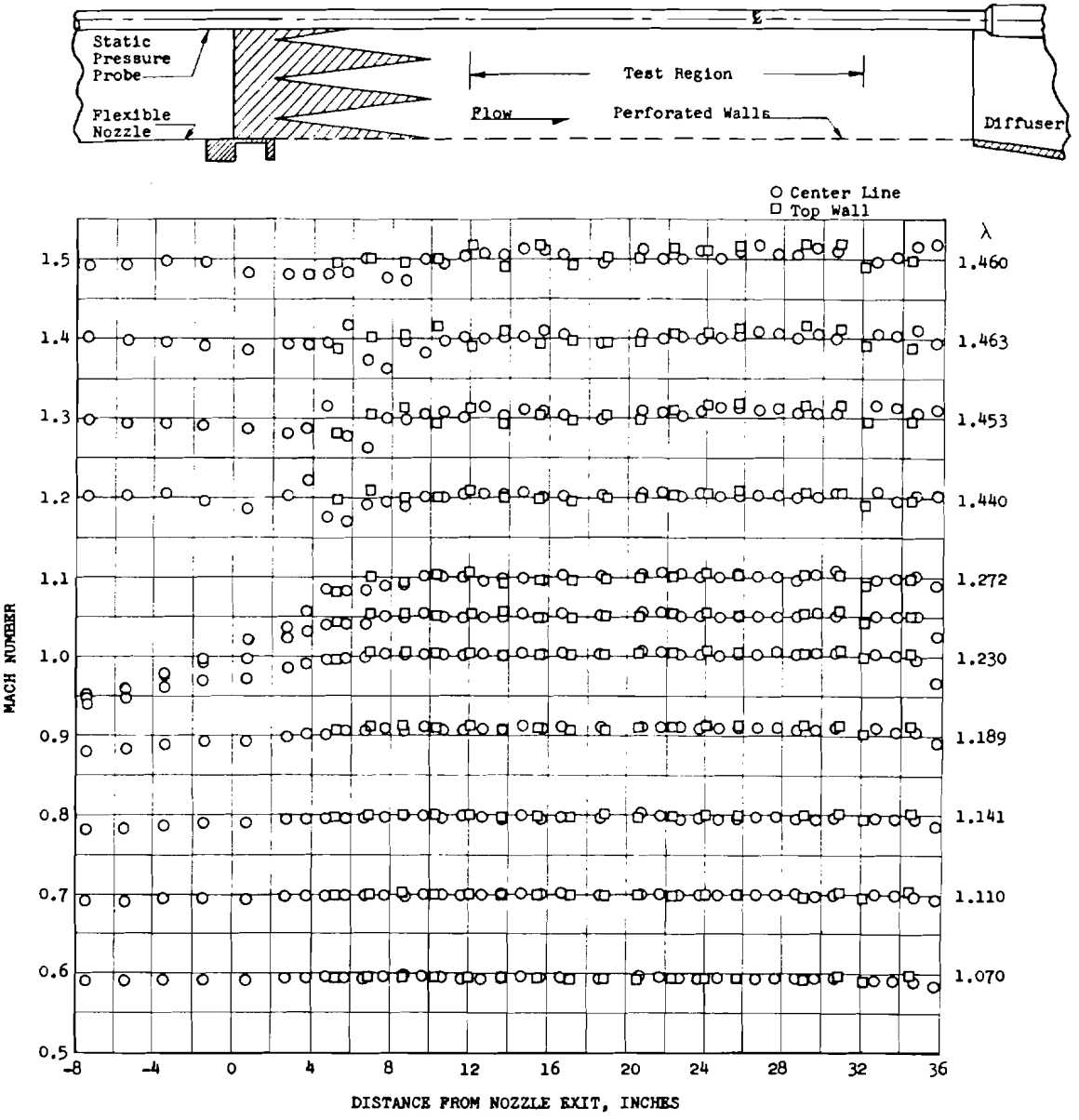

e. $\theta_w = -10$ min

Fig. 9 Continued

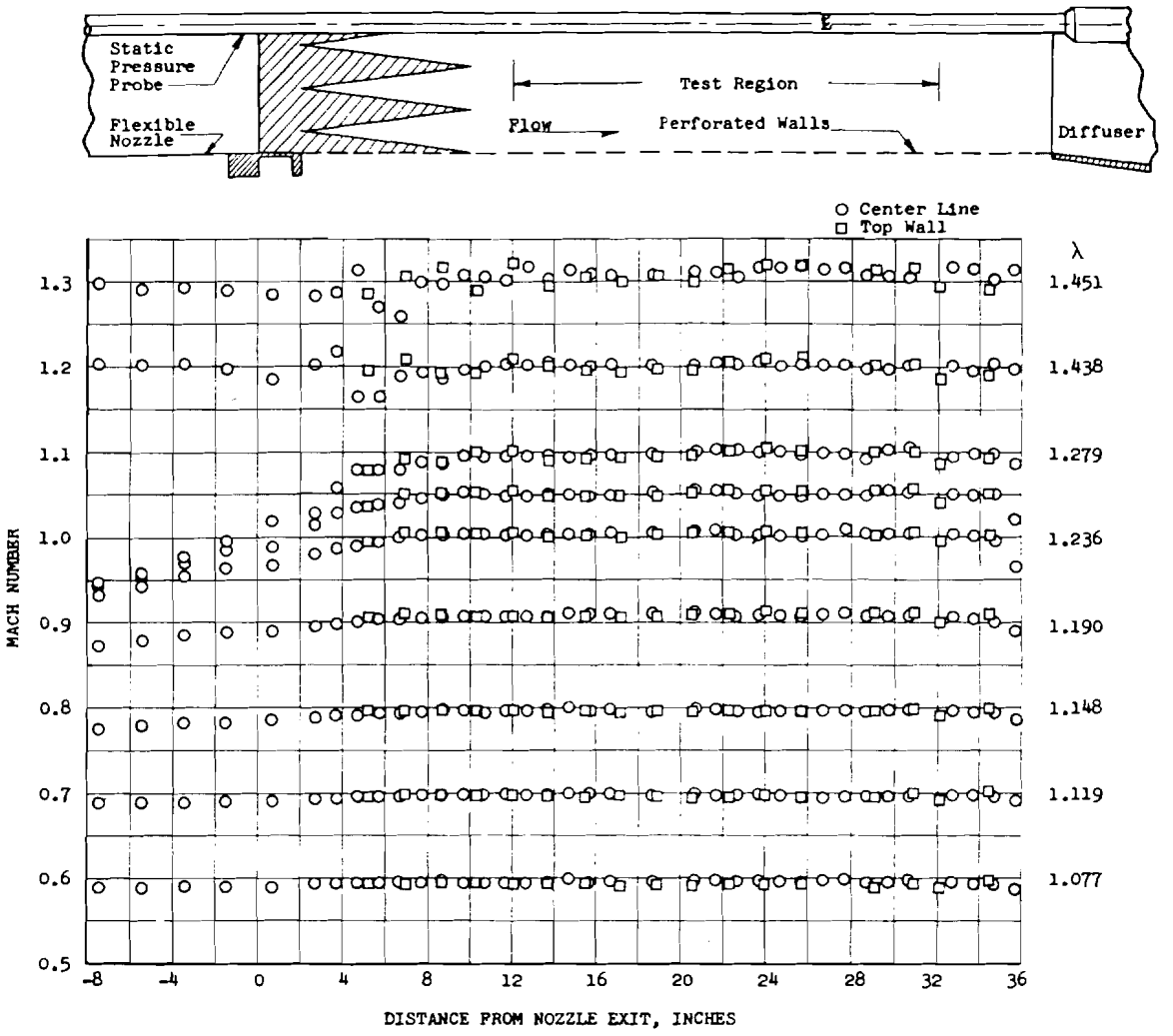

f. $\theta_w = -20$ min

Fig. 9 Continued

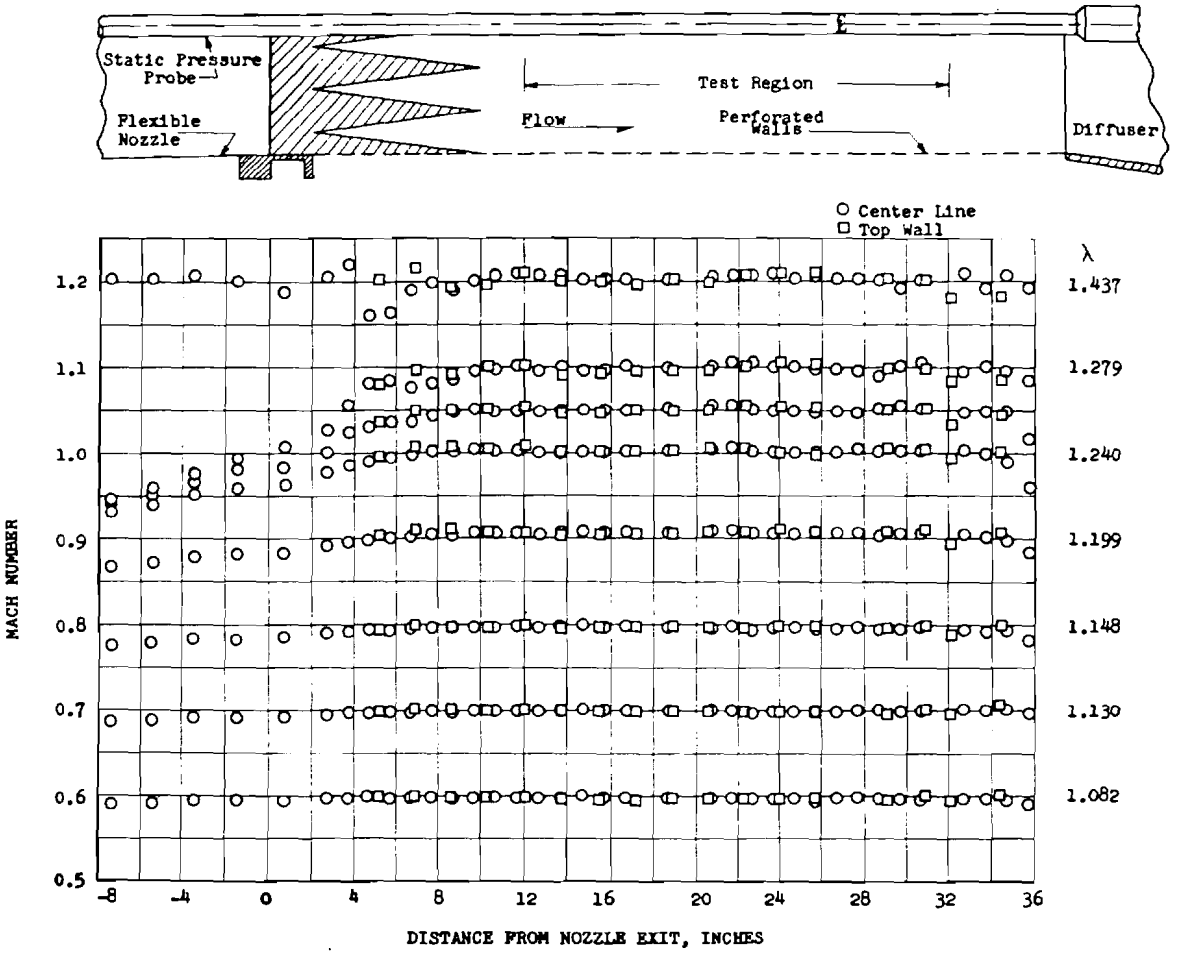

g. $\theta_w = -30$ min

Fig. 9 Continued

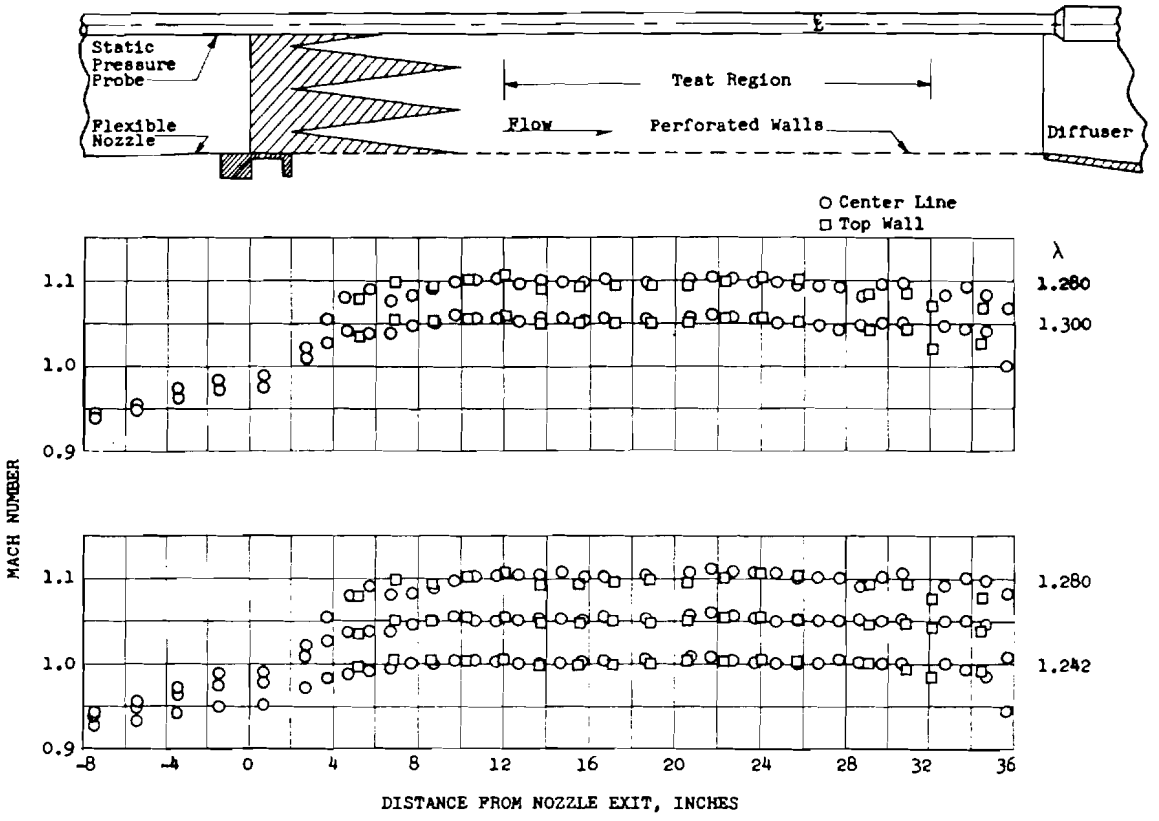

h. θ_w = −40 and −50 min

Fig. 9 Concluded

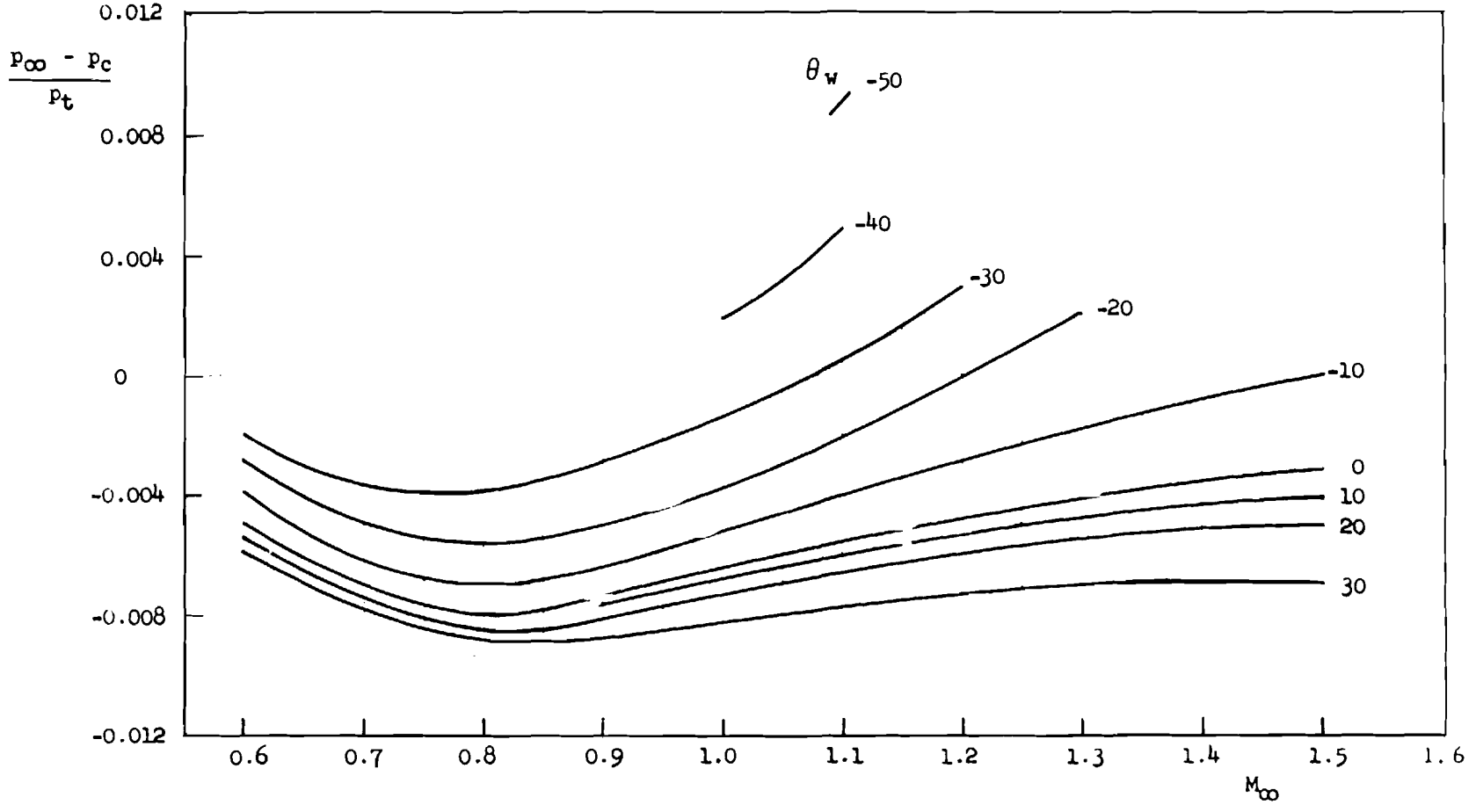

Fig. 10 Plenum Chamber Calibration Factors as a Function of Mach Number for Several Wall Angles

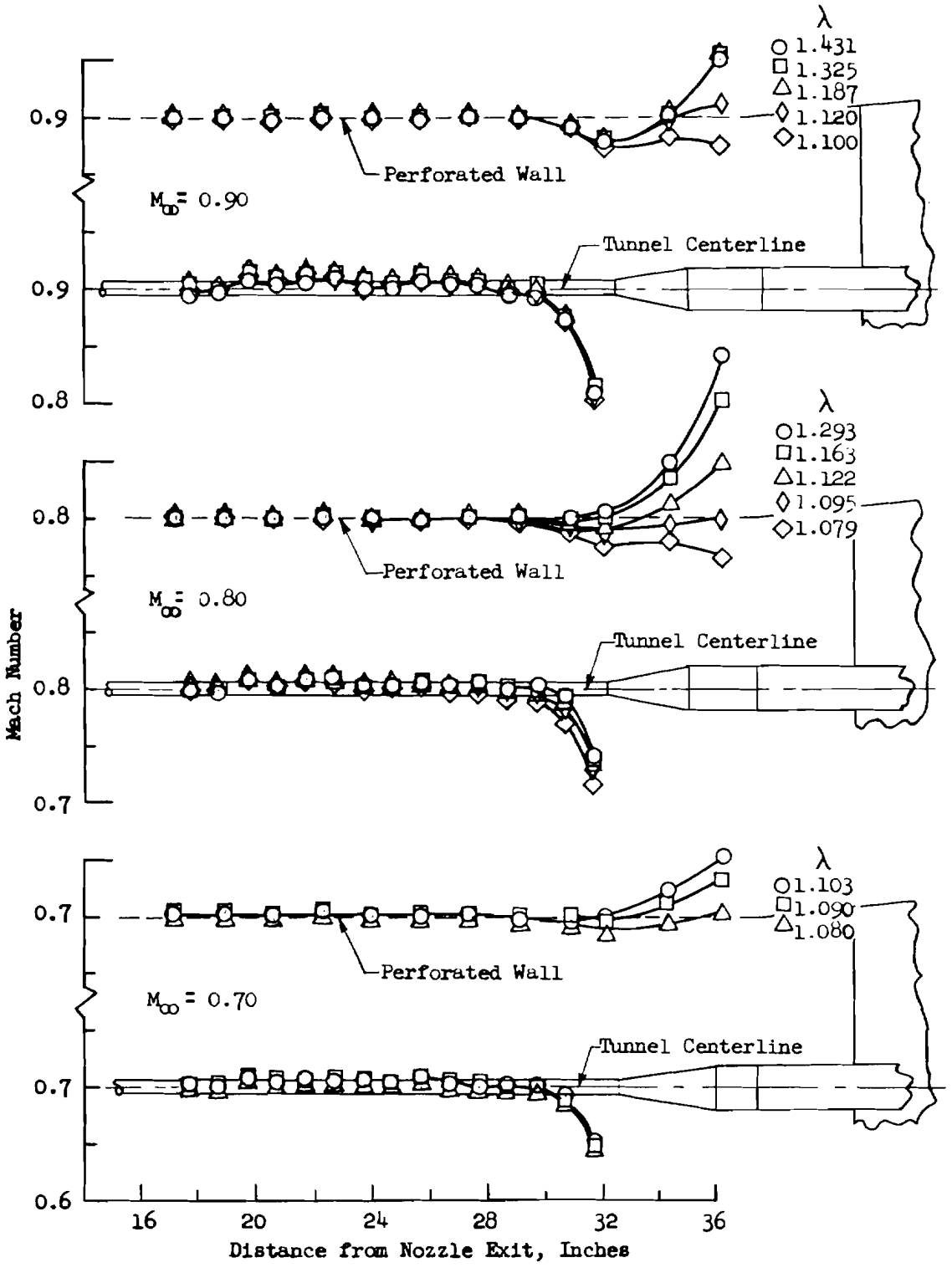

a. M_∞ = 0.70, 0.80, and 0.90

Fig. 11 Effects of Tunnel Pressure Ratio Variations on Mach Number Distributions near the Downstream End of the Test Section

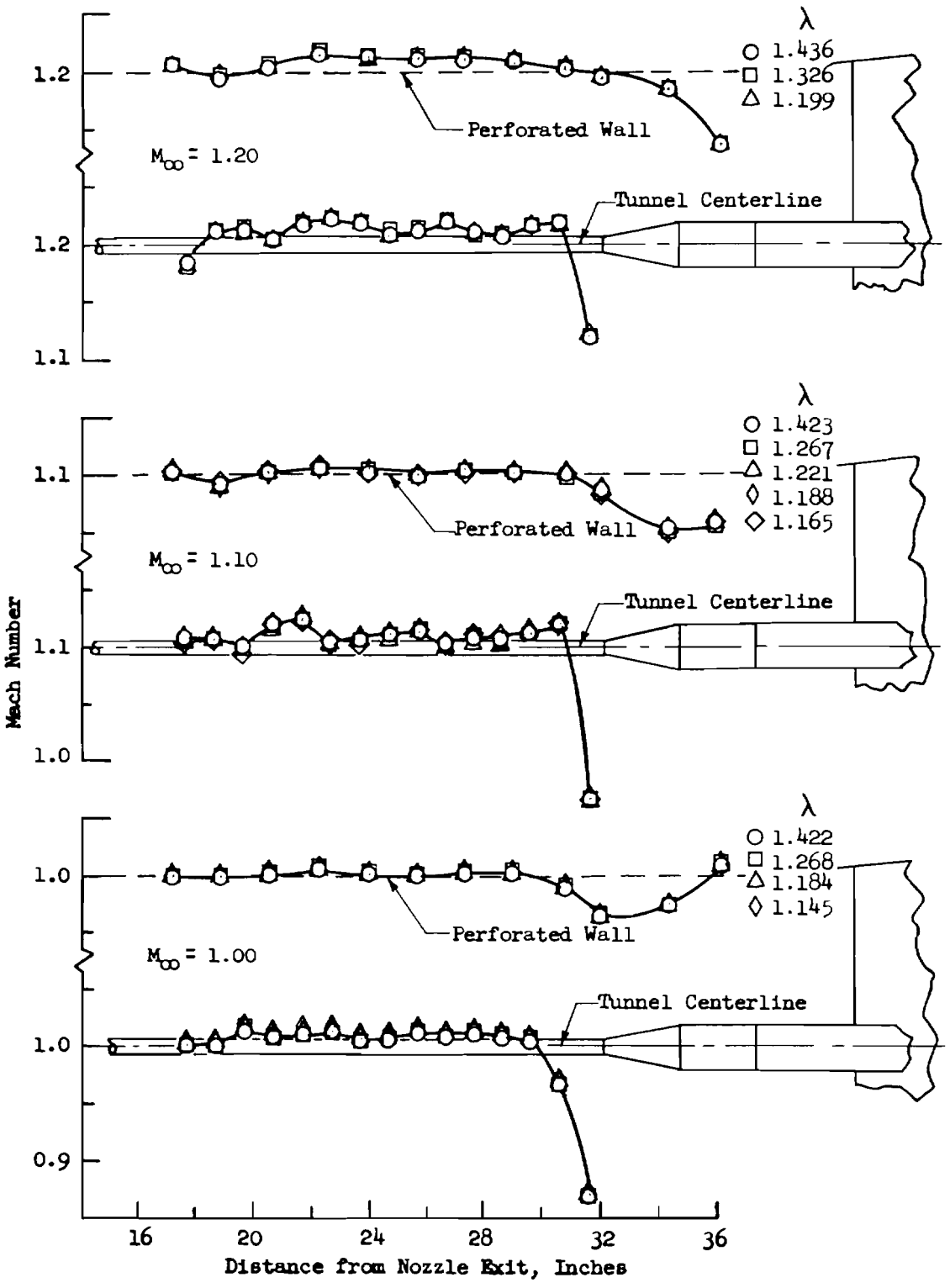

b. M_∞ = 1.00, 1.10, and 1.20

Fig. 11 Continued

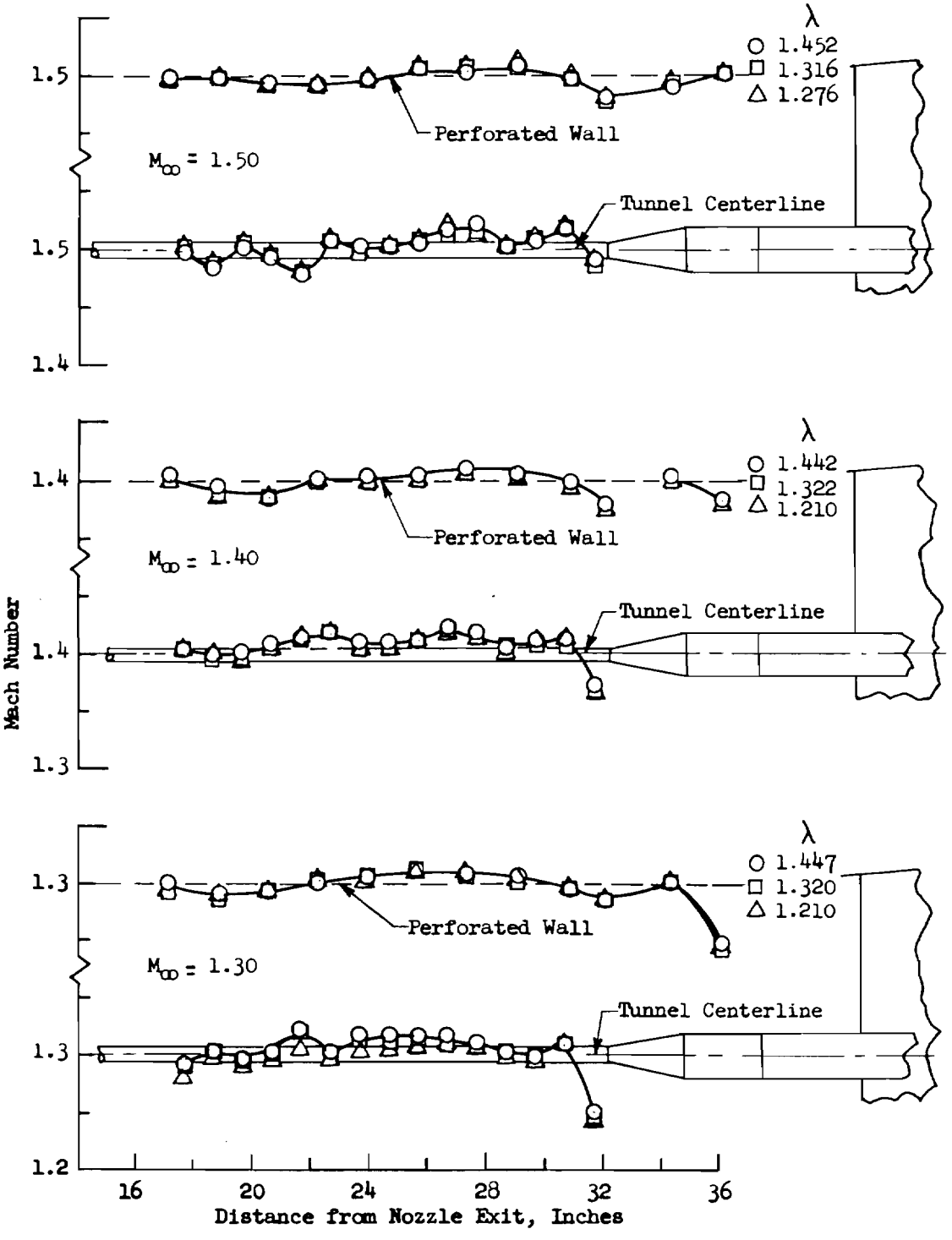

c. M_∞ = 1.30, 1.40, and 1.50

Fig. 11 Concluded

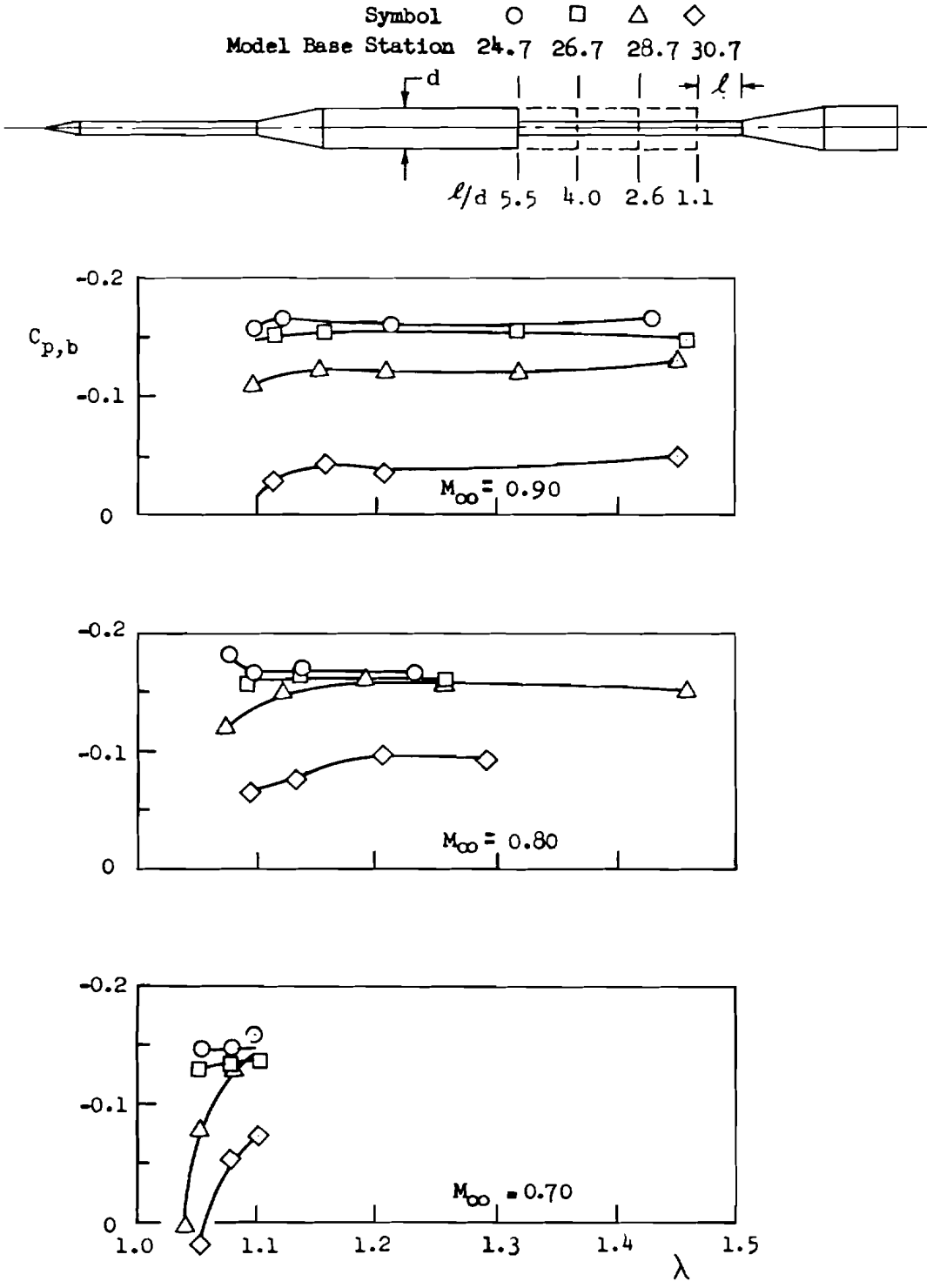

a. M_∞ = 0.70, 0.80, and 0.90

Fig. 12 Effects of Tunnel Pressure Ratio Variations on Base Pressure Coefficients for Several Model Base Positions

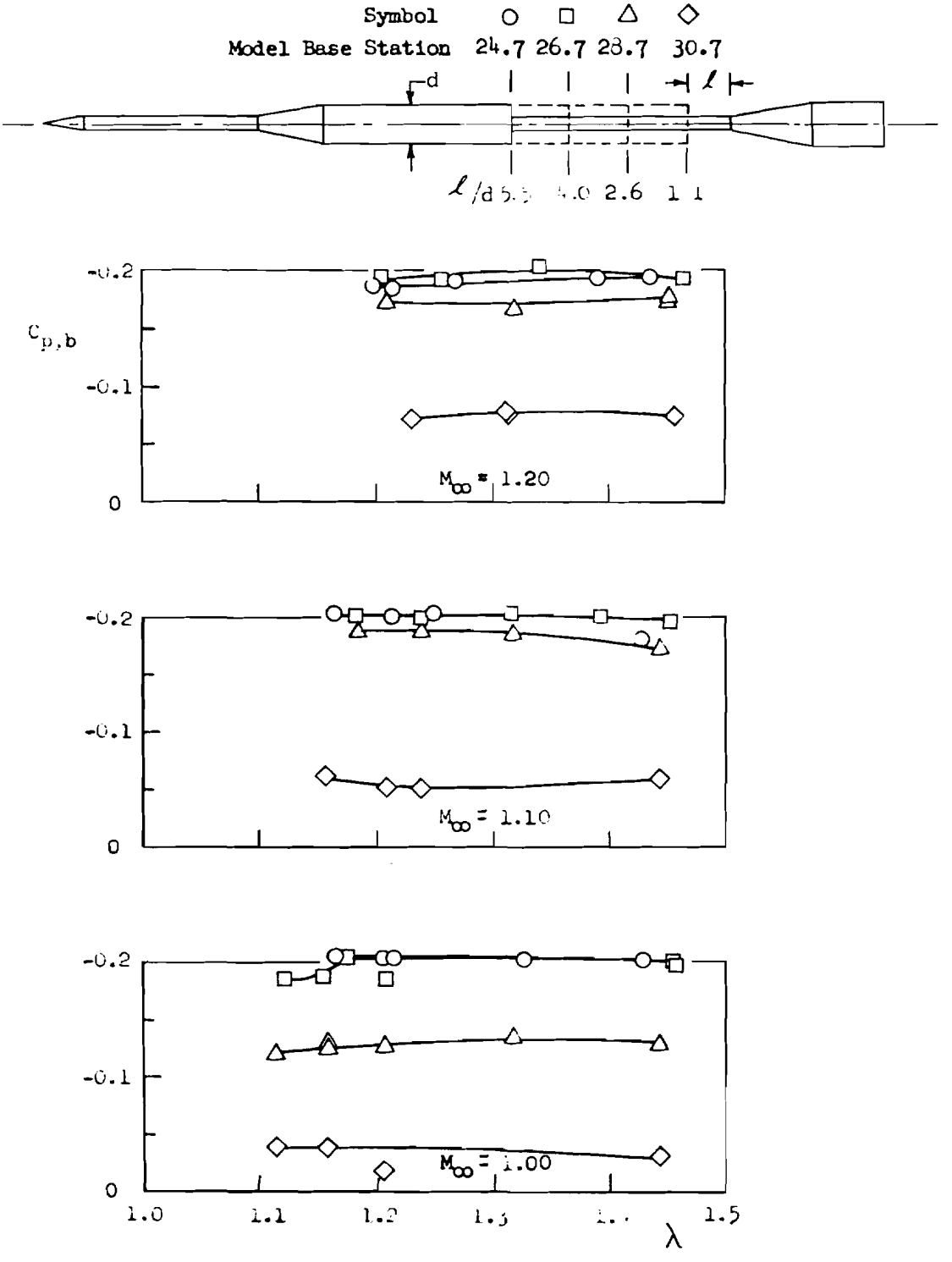

b. M_∞ = 1.00, 1.10, and 1.20

Fig. 12 Continued

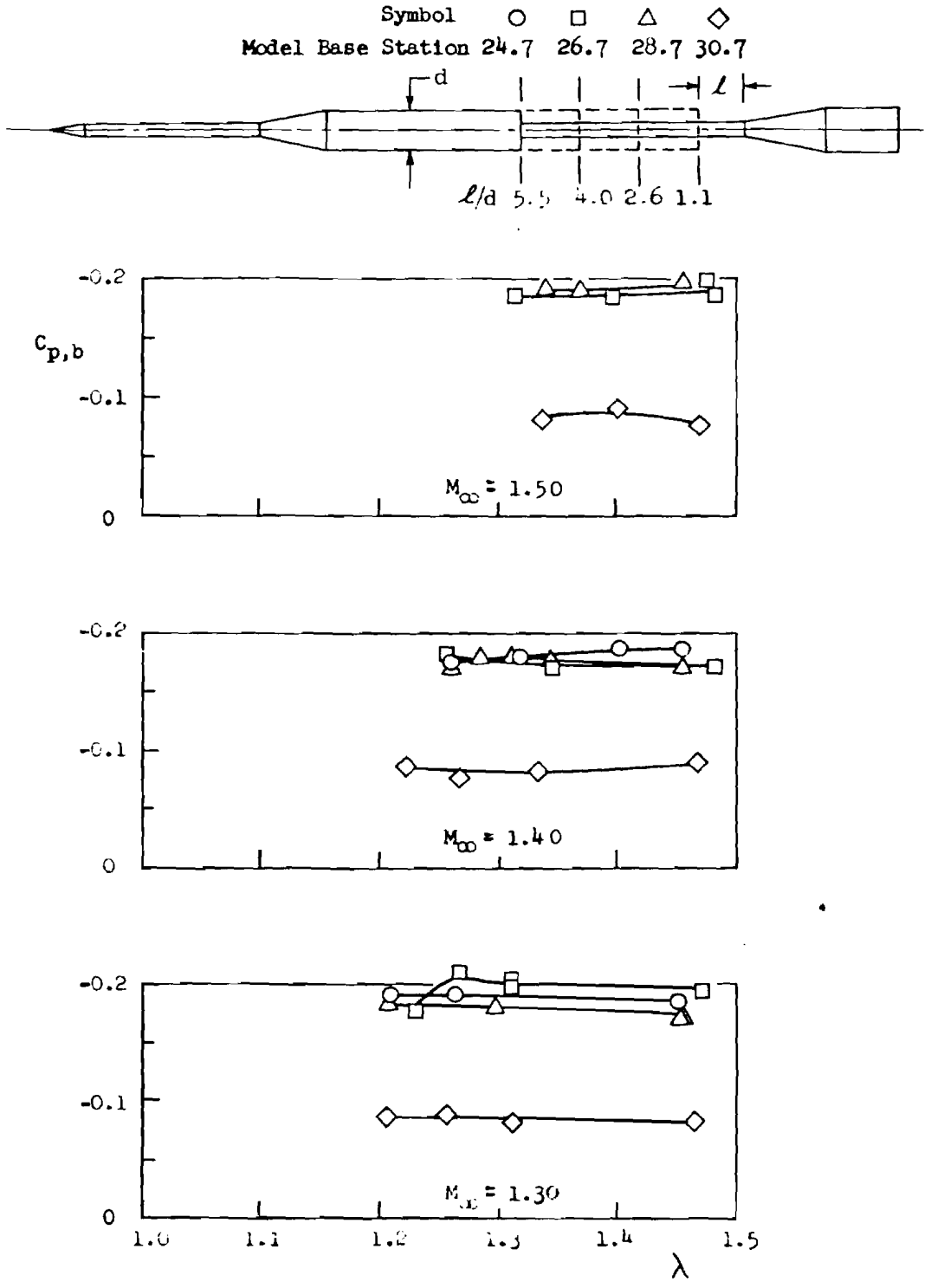

c. M_∞ = 1.30, 1.40, and 1.50

Fig. 12 Concluded

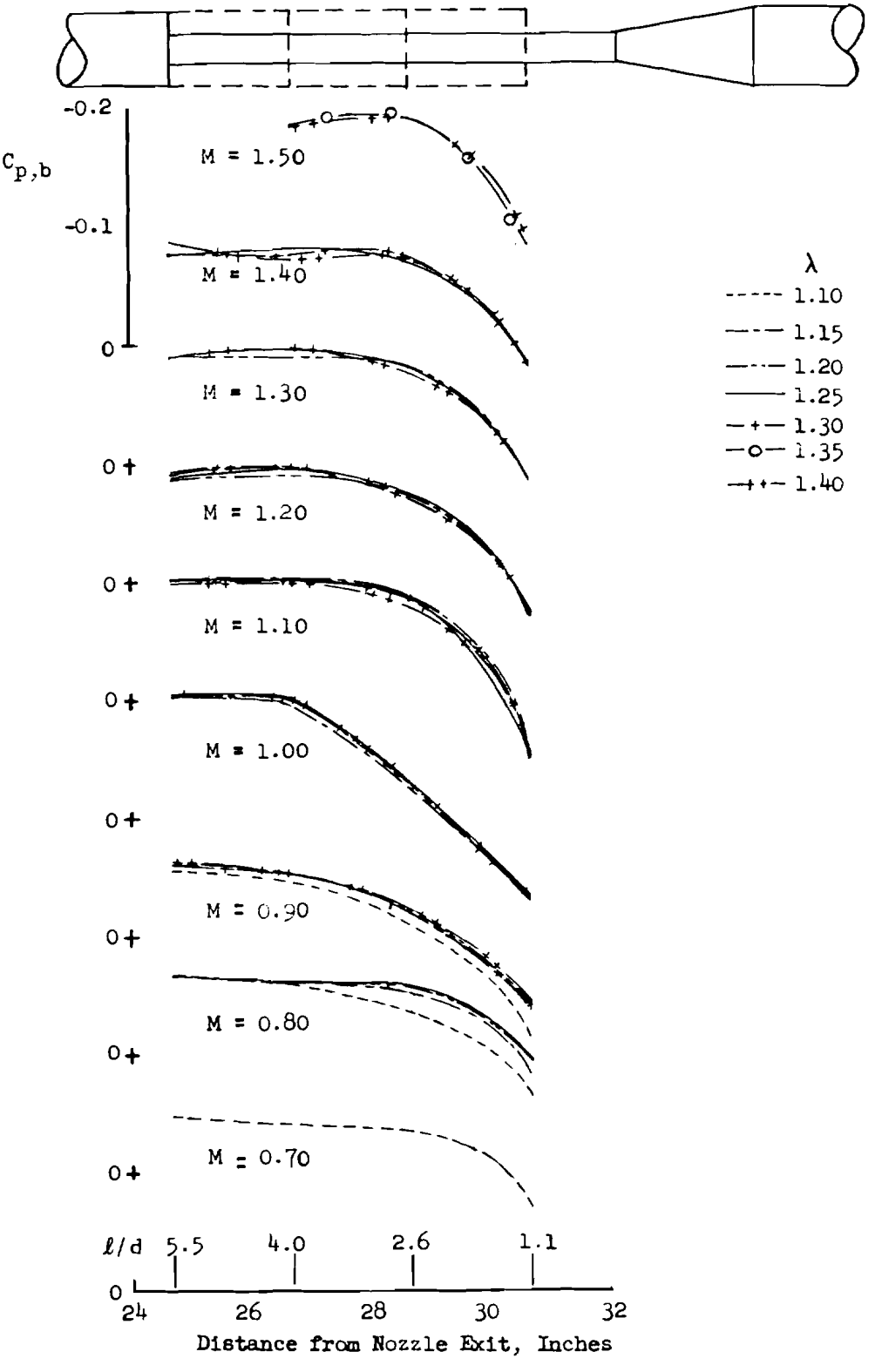

Fig. 13 Variations in Base Pressure Coefficient as a Function of Model Base Position for Several Tunnel Pressure Ratios; Mach Numbers from 0.70 to 1.50